

Modal Analysis for Delamination Detection in Composite Laminates using Laser Doppler Vibrometer and FEA

Wagh Yogesh Shivaji

A Thesis Submitted to
Indian Institute of Technology Hyderabad
In Partial Fulfillment of the Requirements for
The Degree of Master of Technology



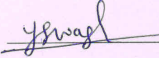
भारतीय प्रौद्योगिकी संस्थान हैदराबाद
Indian Institute of Technology Hyderabad

Department of Mechanical and Aerospace Engineering

June 2015

Declaration

I declare that this written submission represents my ideas in my own words, and where ideas or words of others have been included, I have adequately cited and referenced the original sources. I also declare that I have adhered to all principles of academic honesty and integrity and have not misrepresented or fabricated or falsified any idea/data/fact/source in my submission. I understand that any violation of the above will be a cause for disciplinary action by the Institute and can also evoke penal action from the sources that have thus not been properly cited, or from whom proper permission has not been taken when needed.

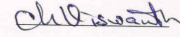

(Signature)

Wagh Yogesh Shivaji
(Wagh Yogesh Shivaji)

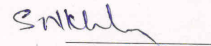
ME13M1018
(Roll No.)

Approval Sheet

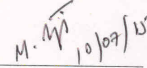
This Thesis entitled Modal Analysis for Delamination Detection in Composite Laminates using Laser Doppler Vibrometer and FEA by Wagh Yogesh Shivaji is approved for the degree of Master of Technology from IIT Hyderabad



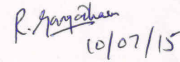
(Dr. Viswanath Chinthapenta, Asst. Professor) Examiner
Dept. of Mechanical and Aerospace Engineering
IITH



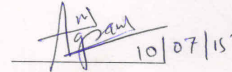
(Dr. Syed Nizamuddin Khaderi, Asst. Professor) Examiner
Dept. of Mechanical and Aerospace Engineering
IITH



(Dr. M. Ramji, Asso. Professor) Adviser
Dept. of Mechanical and Aerospace Engineering
IITH



(Dr. R. Gangadharan, Asst. Professor) Co-Adviser
Dept. of Mechanical and Aerospace Engineering
IITH



(Dr. Anil Agarwal) Chairman
Dept. of Civil Engineering
IITH

Acknowledgements

I would like to thank my adviser Dr.M.Ramji for giving me such opportunity to work on this area, also for giving me continuous motivation throughout my work. I wish to thank Dr.R.Gangadharan for his guidance and sharing his vision of the Structural Health Monitoring concepts and provided many ideas at all stages of this research effort. Exchange of ideas with Dr.R.Gangadharan throughout the research effort were crucial to the successes reported in this thesis. My lifelong dreams are coming true through the help of all my teachers and colleagues. I want to express my thanks to my IITH friends for their constant support and encouragement throughout this work. I would like to thank Dr. Ashok Kumar Pandey for giving me permission to utilise the Vehicle Dynamics Lab and special thanks to Mr. Prasant kambli for teaching me LDV equipment. I want to express my thanks to workshop members, especially Mr.A.Pravin Kumar, Mr.Pramod K. for helping me in fabrication of composite specimens throughout this research work.

Dedication

Dedicated to
My Mother, Sisters and My Teachers

Abstract

Nowadays, detection of delamination is become a major task for utilization of composite materials for structural applications. Vibration based structural health monitoring technique is used for detecting the delamination present in the composite structure. In this research an experimental and numerical approach is developed for detection of delamination in composite materials. The experimental results are presented for the application of modal analysis technique applied to GFRP composite beams containing delamination type of damage. Changes in natural frequencies and mode shapes are found using Laser Doppler Vibrometer and validated with 3-D FE models for comparison with the obtained experimental results. To detect and locate delamination type of damage, vibration based structural health monitoring (SHM) technique is implemented on composite beam structures. Damages in a structure may alter its modal parameters such as natural frequencies and mode shapes. Since, modal parameters are the function of structural properties such as stiffness, therefore changes in modal parameters occurs due to loss in stiffness. Due to presence of localized delamination modal characteristics do change. Thus, finding the modal parameters of the structure with delamination is essential to predict its location. For locating delamination, damage detection algorithms are applied. Further damage location is estimated by applying damage detection algorithms.

Contents

| | |
|--|-------------|
| Acknowledgements | iv |
| Abstract | vi |
| Nomenclature | viii |
| 1 Structural Health Monitoring | 1 |
| 1.1 Introduction of SHM to Composites and Damages | 1 |
| 1.1.1 Importance of Vibration based Structural Health Monitoring | 2 |
| 1.1.2 Current Damage Detection Techniques Available | 3 |
| 1.2 Motivation | 4 |
| 1.3 Literature Survey | 5 |
| 1.4 Scope and Objective | 6 |
| 1.5 Thesis Layout | 6 |
| 2 Laser Doppler Vibrometer | 8 |
| 2.1 Introduction to Laser Doppler Vibrometer | 8 |
| 2.1.1 Theory | 8 |
| 2.1.2 Doppler Effect | 8 |
| 2.1.3 Heterodynamic Interferometry | 9 |
| 2.2 Experimental Modal Analysis using LDV | 10 |
| 2.3 Vibration Test | 10 |
| 2.3.1 Specimen Fabrication | 13 |
| 2.3.2 Testing Parameters | 14 |
| 2.4 Results and Discussions | 16 |
| 2.4.1 Natural Frequencies and FRF | 16 |
| 2.4.2 Experimental Mode Shapes | 19 |
| 2.5 Closure | 24 |
| 3 Finite Element Analysis and Modal Study | 25 |
| 3.1 Introduction | 25 |
| 3.2 Finite element modeling | 25 |
| 3.3 Delamination Modeling | 26 |
| 3.4 Results and Discussions | 26 |
| 3.4.1 Validation of FE results with analytical results | 26 |
| 3.4.2 Validation of FE results with Experimental results | 28 |

| | | |
|----------|--|-----------|
| 3.5 | Damage Detection Algorithms based on Curvature Mode shapes | 36 |
| 3.5.1 | Mode shape (MS) damage index | 37 |
| 3.5.2 | Mode shape slope (MSS) damage index | 37 |
| 3.5.3 | Mode shape curvature (MSC) damage index | 37 |
| 3.5.4 | Mode shape curvature square (MSCS) damage index | 37 |
| 3.6 | Damage Location | 40 |
| 3.6.1 | Curvature Damage Index | 40 |
| 3.7 | Closure | 43 |
| 4 | Conclusion and Recommendations for Future Work | 44 |
| 4.1 | Concluding Remarks | 44 |
| 4.1.1 | Modal Analysis | 44 |
| 4.1.2 | Damage detection Algorithms | 45 |
| 4.2 | Recommendations for Future Work | 45 |
| | References | 46 |

Chapter 1

Structural Health Monitoring

1.1 Introduction of SHM to Composites and Damages

Structural Health Monitoring [1] is the multidisciplinary process of implementing damage detection strategy for engineering structures. Whether the structure is affected by any damage or not, this current state of the structure can be determined by extracting the damage parameters. Structural Health Monitoring (SHM) involves continuous monitoring of the structure over a period of time. SHM characterizes four major damage identification steps such as verification of presence of damage, determination of location of damage, estimation of damage severity and fourth one is prediction of remaining life of the structure. This research focuses on detection and location of damage. Composite material [2] is defined as a combination of two or more visibly distinct constituents or phase separated by two distinct interfaces. As a result, they offer a desirable combination of properties based on the principle of combined action to meet a particular requirement which may not be possible if any one of the constituent is used alone. One of the constituents is called as reinforcement and the one in which it is embedded is known as matrix. Composite materials have a high specific strength and stiffness with a relatively low density. This makes them extremely useful in applications where weight plays an important role such as aircraft, automobiles, civil structures, wind turbines, and sporting goods etc. These materials can exhibit unconventional and complex types of damage, like transverse cracks and delaminations. These damage scenarios are often invisible, which can severely influence the structural performance of a component, and hence tremendously decrease its service life. For that periodic inspections are required to ensure the structural integrity of a component during its service life. Structural health monitoring (SHM) technologies propose a promising alternative and involve the continuous monitoring of a structure. Internal damages such as delamination, fiber breakage and matrix cracks are caused easily in the composite laminates under external force such as foreign object collision which causes barely visible impact damage (BVID). Out of which delamination is a more severe damage which can be induced by transverse impact, can cause reduction in the strength and stiffness of the materials even if the damages are small in size. There is a growing need for continuous monitoring of structures made of advanced composites to avert catastrophic failures and to provide confidence for the rapid introduction of these high performance and heterogeneous materials into service. The dynamic responses of structure offer unique information on defects inside the structure. Since, changes in the physical properties of the structures due to damage can alter the

dynamic responses such as natural frequencies, modal damping and mode shapes. These changes in physical parameters can be extracted to estimate damages in the structure by experimental modal analysis.

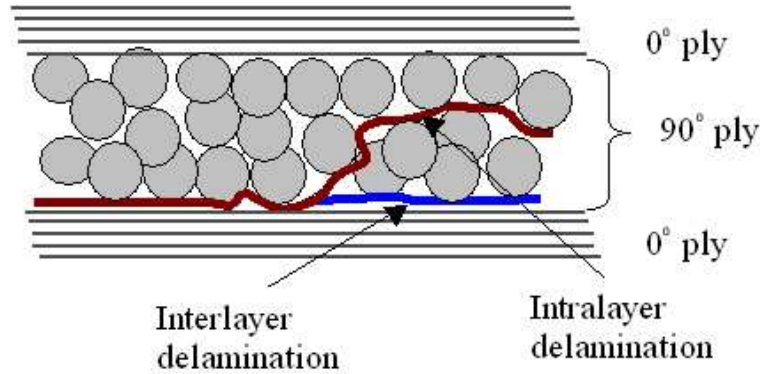


Figure 1.1: Diagram of Internal Delamination

Delamination is a type of damage that generally occurs by transverse cracking in individual plies as shown in Fig. 1.1. This damage type is a debonding between individual plies of a laminate which is nothing but the ply separation. The crack runs against in a plane parallel to the fibers, but at the interface between two layers. Delaminations are hardly visible on the surface, since they are embedded within the composite structure. This makes them barely detectable during, for example, visual inspections. Although delaminations do not lead to complete fracture, they can seriously affect the mechanical properties of the composite laminate. Delamination significantly decreases the load carrying capacity of a laminate. Fiber related failure in a laminate is mostly accompanied by matrix related damage such as transverse cracks and delaminations. Composite structures are prone to unpredicted failures due to greater complexity of design, high operational loads and longer service life. Composites mainly exhibit four types of damages namely such as fiber breakage, matrix cracking, delamination and debonding. This study, mainly focus on delamination type of damage study. For detection of delamination in composite beams dynamic analysis has been studied. High strength of fibrous composites in the direction of reinforcement is accompanied by a low resistance against interlaminar shear and transverse tension. This may cause delamination leading to initiation and propagation of cracks. Delamination may arise at the fabrication stage itself (e.g., incomplete wetting, air entrapment), during transportation (mishandling, low intensity impacts) and/or during its use (e.g., low velocity impact, bird strikes on aircraft panels). Delaminations present nearer to the surface are greatly affected by local buckling. The presence of delamination significantly reduces the stiffness and strength of the structure and affects critical design parameters. If modified dynamic response of the structure due to damages is closer to the operating frequency range during the use, it may cause serious damage to the structure due to uncontrolled vibration response.

1.1.1 Importance of Vibration based Structural Health Monitoring

Structural Health Monitoring (SHM) [3] is the process of assessing the state of health of a structure and further predicting its remaining life. Vibration based Structural Health Monitoring (SHM) is one of the major tool for maintaining the safety and integrity of the structures such as aerospace,

automotive and civil structures [4]. So, there is a need to identify reliable non-destructive damage detection for the development of health monitoring techniques as invisible or undetected damage may grow and causes to structural failure. The challenge is to interpret the changes of the physical parameters due to delamination type of damage and correlate them with the corresponding measured modal parameters. Due to the anisotropy of the composite material and the fact that the delamination occurs beneath the surface of laminates increase the complexity of damage assessment in composite structures.

Vibration-based SHM provides an identification method based on modal parameter such as natural frequencies, mode shapes, and frequency response functions (FRFs) are functions of the physical properties of the structures such as stiffness, mass, and modal damping. Therefore, the changes in these dynamic parameters can be used to locate and assess damages. The dynamic behaviour of the structure is function of these physical properties and will therefore directly affected by the presence of damage. The dynamic behavior can be described by time, frequency and modal domain parameters. These three parameters gives an information about the presence of damage. Vibration-based SHM method consists on establishing differences in the modal properties of a structure by using dynamic response data before and after damage. However, one of the most important aspects of vibration-based method is that damage is a local phenomenon and may not significantly influence the lower-frequency response of the structure. The usage of FRF is a good alternative for SHM systems, because structural FRFs may be sensitive to the damages present in the component. In fact, this sensitivity depends on different aspects, such as the size and the location of the damage, as well as the captured mode shape.

1.1.2 Current Damage Detection Techniques Available

The wide variety of nondestructive testing techniques which can be used for damage detection purpose are briefly described here. Here, an overview of the most commonly used nondestructive testing technologies that utilize vibration principles to identify damage are described [5].

Structural vibrations and acoustics (SV)

This group of techniques utilizes the changes in the structural dynamic behavior (e.g. natural frequencies, damping, modes of vibration) of structures caused by damage, significantly alter the structural integrity and therefore the physical properties like stiffness, mass and/or damping. The dynamic behavior of a structure is a function of these physical properties and therefore directly will be affected by damage. The low-frequency vibration based technology provides data that is relatively easy to interpret. More complex structures can be analyzed with these methods and a relatively large area can be explored at once. The frequency range, and hence the resolution, is however limited. Using this technique, only relatively severe damage such as delaminations can be identified.

Electro-mechanical impedance (EMI)

The electro-mechanical impedance technique is essentially a structural vibration technique, but is usually considered to be a separate one. This approach uses changes in the mechanical impedance of the structure to identify damage. The mechanical and electrical domain are connected by means

of a piezoelectric element that is attached to the structure. An excitation signal is applied to the piezoelectric element. The applied voltage and the current that flows through the element are measured simultaneously to determine the mechanical impedance. This approach is of low cost and easy to apply, but generally lacks the physical interpretation of the measured deviations.

Acoustic emission (AE)

The acoustic emission technique utilizes the transient stress waves generated by a local source. The variety of sources comprises, an actively growing defect in a structure under operational loading such as mechanical impact. The emitted stress waves propagate through the surface and are recorded by a network of sensors. Unlike most other techniques, Acoustic Emission does not require an active excitation. Other advantages include the fast inspection using a limited number of integrated sensors as well as the ability to find out between developing and stagnant defects. A drawback of it is that a continuous operation of the system needs to be guaranteed. One of the key difficulties is to find out the signals from other environmental noise while the structure is in operation.

Ultrasonic testing (UT)

Ultrasonic testing is similar to the acousto-ultrasonics technique. The method also utilizes high frequency ultrasonic waves to characterize a specimen. The main difference lies in the traveling direction of the ultrasonic waves, which is usually normal to the surface of the specimen and this technique is applicable to detect crack problems and is not suitable for delamination type of problems.

Laser Doppler Vibrometer (LDV)

Scanning Laser Doppler Vibrometers(LDVs) [6, 7] are commonly used in the vibration community to measure the velocity of vibrating surface over a broad area of interest. In this technique, the laser light reflected back to sensor from the vibrating object is compared to the reference beam and relative change in frequency between reference beam and measured beam will be correlated to obtain the surface velocity of the vibrating object using doppler frequency change. As opposed to the other optical techniques one can easily extract transfer function (frequency response function, FRF). As change in FRF gives information of healthy and damage structure. Further it is non-contact and non-mass loading vibration measurement system.

1.2 Motivation

Nowadays, composite materials are being used in day to day life, such as aircraft structures, automobiles, sporting goods etc. In case of aircraft structures made of composite materials there are certain damage scenarios such as during flight due to bird strike or impact of foreign object like barely visible impact damage(BVID), affects its service life. So there is a need as and when these kind of damages happens. Objective of this work is to detect damage present in structure and further find the damage location in order to avoid the catastrophic failure. In this study the goal is to advance the state of the art of SHM techniques through the use of non-contact Laser Doppler

Vibrometer technique to capture the structural dynamic responses to detect small defects like delamination. Further, a numerical model is developed to exactly capture damage location involving well defined damage measures. Structural health monitoring (SHM) technologies propose a promising alternative and involves continuous monitoring of a structure by employing a nondestructive testing (NDT) approach based on an integrated sensor system. As the damage mechanisms for composite materials are more complex such as intra-ply failures e.g., fibre fractures and polymer matrix cracks and delaminations i.e. separation between plies can occur, leading to reduced structural integrity. Therefore, a need for damage detection in composite materials.

1.3 Literature Survey

The application of modal analysis is one of the most used approaches, and it is based on the frequency response function (FRF) for detecting damage in structures as observed, in the past, by Cawley and Adams [8, 9] simply used the frequency changes for different modes to detect the damage in composite structure and location of damage zone is identified where the theoretically determined ratios of frequencies and experimental values are equal. Tracy and Pardoen [10] found that the natural frequencies of a composite beam were affected by the size and damage location and delamination has no more than twenty percent effect on the first four natural frequencies of the delaminated beams compared to the undamaged composite beams. Pandey et al.[11] showed that irregular of mode shape is significant for relatively large damage. M.J.Parvier and M.P.Clarke et al.[12] have studied Experimental techniques for investigation of the effects of impact damage on carbon-fiber composite. Therefore, Farrar and Doebling [13] presented some methods to assess the vibration response of the structure in order to detect, localise and quantify the damage. So, these methods have used the differences in natural frequencies and mode shapes between undamaged (healthy) and damaged structure due to modifications of the structural stiffness, mass and damping. However, the greatest challenge is related to the damage sensitivity. Thus, vibration-based techniques are often considered global methods. Hanagud et al.[14] have proposed a method of delamination coefficients to study the existence of delamination in composite plates without visualizing the mode shapes. Higher values of these coefficients are used as quantitative measure of delamination in the composite plates.. Zou et al.[15],which presents a review of vibration-based techniques that rely on models for identification of delamination in composite structures by developing theoretical methodology of delamination beam. Kessler et al.[6] in their pioneer work have used Laser Doppler Vibrometer for observing changes in natural frequencies and mode shapes for various types of damages such as impact, cut-out and delamination in graphite-epoxy composite beams. Frequency response based methods are found to be more reliable than mode dependent damage detection methods as coalescence of higher frequency modes makes it difficult to analyse the true nature of the damages. Sunghee Lee, Taehyo Park and George Z. Voyiadjis et al.[16] have proposed Vibration analysis of multi-delaminated beams. An analytical formulation is proposed and studied for the vibration analysis of the composite beams with arbitrary lateral, longitudinal, and both multiple delaminations. Experiments are performed for the case of a single delamination and finite element analysis is conducted for multiple delaminations. Christian N. Della, Dongwei Shu* [17] presents a review on vibration of delaminated delaminated composite laminates, they have provided survey on various analytical models and numerical analyses for the free vibration study of delaminated composite beams. Also they have presented basic

understanding of presence of delamination on natural frequencies and mode shapes of composite laminates. Lestari and Qiao [4] have developed Curvature Mode Shape-based Damage Assessment of Carbon/Epoxy Composite Beams. A combined analytical and experimental damage assessment method using curvature mode shapes is developed. The curvature mode is selected due to its sensitivity to the presence of the damage and the localized nature of the changes. An analytical relationship between the damaged and the healthy beams is formulated, for which the effect of damage in the form of stiffness loss is accounted. The relationship between healthy and damaged beam is used to estimate the extent of damage from the experimentally identified changes in structural dynamic characteristics. Tita et. al [18], studied the failure mechanisms are dependent on the geometry, laminate thickness, stacking sequence of plies, energy level and boundary conditions. Rucevskis* and Wesolowski [19] have identified damage in a beam structure using mode shape curvature squares method by developing the damage detection algorithm. The applicability of mode shape curvature squares determined from only the damaged state of the structure for damage detection in beam structure is studied. Fan and Quiao [20] carried out the work were focus on flat beams and plates and they have identified the damage identification algorithms in terms of signal processing. They have observed that most of the mode shape-based and curvature mode shape-based methods focus on the damage localization. Obinna K*. Ihesiulor, Krishna Shankar, Zhifang Zhang and Tapabrata Ray [21] studied the existence of delaminations changes the vibration characteristics of laminates and hence such indicators can be used to quantify the health characteristics of laminates and detect potential risk of catastrophic failures.

1.4 Scope and Objective

Over the past decades, in aerospace structure of Boeing Dreamliner 787 and Airbus A380 some invisible damages have occurred during its service due to collision of foreign object such as bird strike which causes damages like barely visible impact damage (BVID). Mostly BVID results in matrix cracking and sub surface delamination. Detection of such barely visible impact damage is a cumbersome and a critical task in aircraft maintenance. The structural health monitoring technique mostly applied for detection of delamination damage are based on vibration based SHM. Objective of this study is to detect and locate the simulated delamination damage present in composite lamiate using modal data obtained from Laser Doppler Vibrometer and validate it with FEA model. The scanning laser vibrometer is a practical technique to study the vibration characteristics of structure. Here, a new procedure has been developed to accurately predict the damage location using curvature information. The model shape depend on the stiffness of the structure and hence one can use that information damage identification based on the obtained modal data from LDV measurements.

1.5 Thesis Layout

Chapter 1 gives an introduction to structural health monitoring being applied to composite structures, literature survey of LDV applications for mode shape extractions has been carried out. Motivation, scope and objectives including thesis layout for the work carried out is discussed at the end.

Chapter 2 is describes experimental technique and whole chapter is dedicated to Laser Doppler

Vibrometer technique, in that theory of LDV, interferometry, working principal and experimental procedure to extract modal data has been discussed. Vibration test on various configuration on composite laminated beams has been carried out. Experimental modal data and frequency response function obtained from LDV has been discussed or both healthy and damaged composite specimens.

Chapter 3 contains Finite Element Analysis based Modal study where 3D models are created and studied using standard FEA package for both healthy and damage cases. Delamination is introduced using contact element and further modal study is carried out. After extracting modal information prediction of damage location is carried out using the derived curvature field by appropriately estimating few well defined damage indices.

Chapter 4 presents conclusion and recommendations for future work.

Chapter 2

Laser Doppler Vibrometer

2.1 Introduction to Laser Doppler Vibrometer

2.1.1 Theory

Laser Doppler Vibrometer (LDV) is a Laser based non-contact vibration measurement technique. It consists of measuring scanning head which is capable of measuring the movements in 1D i.e out of plane direction which provides full information of the out of plane displacement component. It is a precision optical transducer used for determining vibration velocity and displacement at a fixed point of the vibrating object. The technique works on the principle of Doppler effect and interferometry, by sensing the frequency change of back scattered light from a moving surface of object. The LDV system software controls the entire measurement process with graphical user interface. The PSV 9.0 acquisition system has the provision for input channels which can be used for simultaneous acquisition of data from power amplifier, electrodynamical shaker etc. Transfer function which is nothing but the frequency response function (FRFs) between any of the input channels connected to the system can be obtained. Signal generator card contained in the system is used for generating excitation signals in the frequency range of 0-80 kHz. LDVs can measure vibrations up to 40 kHz range linear phase response and high accuracy. Applications of LDV includes modal analysis of automotive parts, car bodies and aircraft panels etc.

2.1.2 Doppler Effect

Doppler Effect is the change in the frequency or wavelength of emitted waves as the source for an observer the wave moves relative to its source. The change in natural frequency observed depends on the speed and direction of travel of both source and observer. Helium-Neon (He-Ne) Laser beam having wavelength of 633 nm ($\lambda = 633nm$) is made to incident on the vibrating surface and the reflected Laser light from the vibrating surface is detected by the vibrometer scanning unit. Incident and reflected beams are made to interfere on the detector as shown in Fig. 2.1 by suitable arrangement. The vibrating surface of an object induces the shift in frequency on the reflected light received by the He-Ne laser. According to Vibrometer optics law the shift in Doppler frequency is given as

$$f_D = \frac{2V}{\lambda} \quad (2.1)$$

where f_D is the frequency shift in the reflected beam, V is the velocity of specimen surface and λ is the wavelength of He-Ne laser.

2.1.3 Heterodynamic Interferometry

The Laser Doppler Vibrometer works on the basic principle of optical interference between two coherent light beams such as measurement beam and reference beam. The interference of these two beams is related to the path difference between the measurement and reference beams. If the path difference between the interfering beams is integral multiple of the laser wavelength then constructive interference occurs. The resultant of interfering beams is having amplitude more than amplitude of individual beams. The resultant intensity of laser light is given as

$$I_{total} = I_1 + I_2 + 2\sqrt{I_1 I_2} \cos \left[\frac{2\pi (r_1 - r_2)}{\lambda} \right] \quad (2.2)$$

where I_{total} is the resultant intensity, I_1 and I_2 are the intensities of two interfering laser beams and $(r_1 - r_2)$ is the path difference between the beams. In this case, overall intensity becomes four times the single intensity. If the path difference is odd multiple of half the wavelength then destructive interference occurs where the overall intensity becomes zero. Figure 2.1 shows interference phenomenon in Laser Doppler Vibrometer.

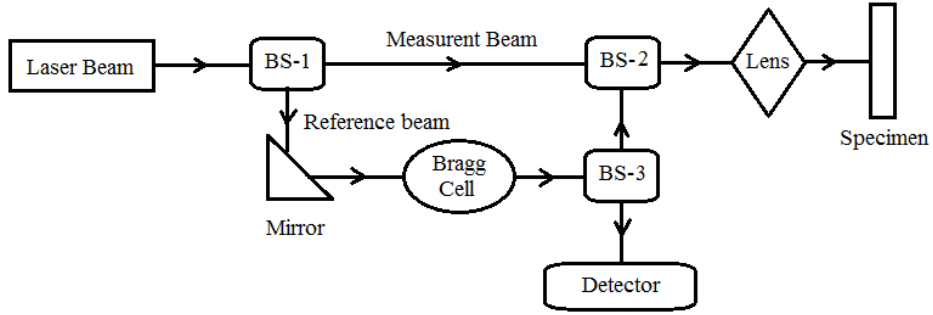


Figure 2.1: Basic Principle of LDV

A He-Ne Laser beam is split by a beam splitter BS1 into a reference beam and a measurement beam. After passing the beam splitter BS2, the measurement beam is focused onto the vibrating surface the specimen. The surface of the specimen must be reflective by applying white spray coating or retro reflective tape. Here, white paint is painted on the specimen surface for better reflection. The reflected beam from the specimen surface is deflected by beam splitter BS2 and is merged with the reference beam by the third beam splitter BS3 and is then directed on to the detector. A Bragg cell is placed in the reference beam to distinguish the direction of movement as it changes the frequency of laser beam. As the path length of the reference beam is constant over time, a movement of the vibrating specimen under consideration generates a dark and bright fringe pattern on the detector. One complete darkbright cycle corresponds to vibrating specimen displacement of exactly half the wavelength of the laser light used. For a He-Ne Laser beam this displacement is 316 nanometers. This change in the optical path length per unit time causes the Doppler frequency change of the measurement beam which is projected on the surface of the specimen.

2.2 Experimental Modal Analysis using LDV

Modal data describe the dynamic properties of a structure and can assist in the design of almost any structure, helping to identify areas where design changes are needed. Natural frequencies and mode shapes associated with corresponding natural frequencies obtained from experimental technique using LDV which describes the dynamic properties of structure. The experimental modal analysis involves measurement of time-domain data, which transform time-domain data into frequency domain-data such as frequency response functions(FRFs) using Fourier's transform, and FRF analysis. The type of FRFs depending upon available sensing devices is used. Here, the FRFs displacements are obtained by using electrodynamic shaker. The data analysis of FRFs includes extraction of modal parameters such as natural frequency and associated mode shape.

The experimental modal analysis was conducted using a Polytec PSV-500 non-contact Scanning Laser Doppler Vibrometer and data was processed using software PSV 9.0 to extract the natural frequencies and modeshapes. The beams were tested in cantilever boundary conditions. The length of the cantilever beam excluding the clamped region is 220 mm while width of the beam is 50 mm. Laser Doppler Vibrometer technique is ideally suited for modal tests because it provides highly precise measurement data without mass loading problems and a high spatial resolution for detailed FEM correlations. The complete data sets can be exported into commercially available software packages for experimental modal analysis as ASCII, MEscape, UNV and others formats.

2.3 Vibration Test

For vibration test to be conducted on Laser Doppler Vibrometer, Figure 2.2 shows the schematic diagram for LDV setup. As shown in the schematic diagram one input signal is given to scanning head from vibrometer controller of the LDV system and another external signal is given to power amplifier for excitation purpose of the specimen. Power amplifier gives excitation signal through BNC connectors to the electrodynamic shaker to vibrate the specimen.

Details of the Test Setup

Composite beams are coated with white spray for the purpose of better reflection. The beams are experimented in cantilever position such as one end is fixed in fixture which is mounted on shaker itself as shown in the Figure 2.3. For the dynamic excitation of the composite beam an electrodynamic shaker(IMV, VE-7144) is used. A power amplifier (IMV, MODEL CE-7144) is connected to the shaker for the purpose of amplifying the excitation signal generated by the LDV system. During the experiment, a periodic chirp signal in the frequency range of 100 Hz to 50 kHz is used for the excitation of the composite beam. Depending upon upto what frequency mode shapes needs to be extracted required frequency range is assigned towards acquisition. For this experiment frequency range of 0-5000 Hz is used, with FFT lines of 3200. Experiment is carried out in two steps. In the first step the beam is excited from 0-5000 Hz with a signal voltage of 10 V. In the second step the beam is excited from 5 -12 m/s^2 with increased amplifier gain in order to excite the high frequency modes.

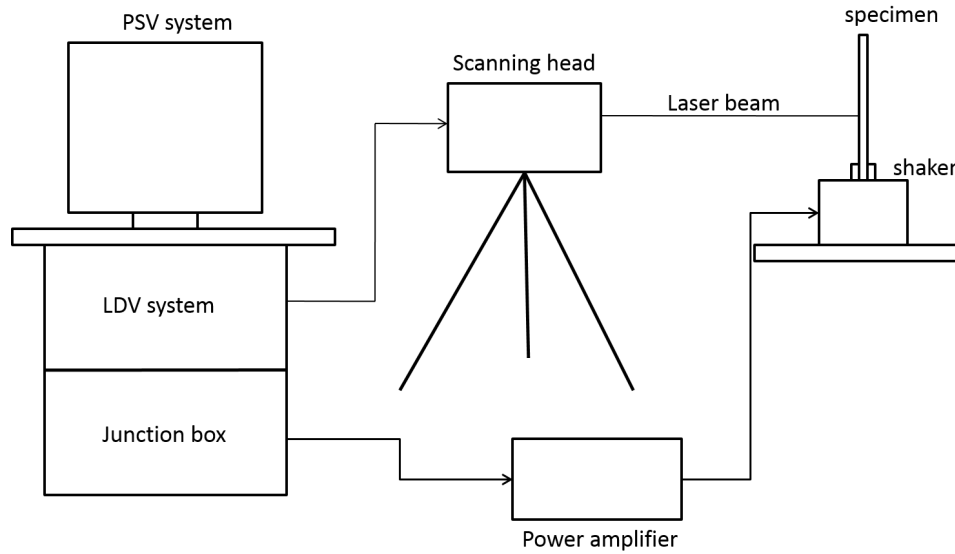


Figure 2.2: Schematic diagram for LDV

Alignment procedure

The 2-D alignment step is carried out to relate the video and scanner coordinate system. This is done by selecting 10-15 points over the scan area and atleast 4 to 5 points should be provided at each side of the specimen. PSV software stores the video coordinates and the scan angles of these points on the scan area and calculates the polynomial interpolation. 2-D alignment step performed for one of the scan heads is shown in Figure 2.4.

Geometry scan

All the scan points in the mesh grid are accessed by the Laser in order to estimate the surface of the specimen. The Laser coincides at each and every scan point on the mesh grid. The accuracy of the surface estimated depends on the previous steps. This step is crucial to obtain the exact simulations of the test surface from the test.

Data Acquisition parameters

Data acquisition parameters such as the excitation signal to be used, frequency range, parameters such as FFT lines and bandwidth, average magnitude of 3, velocity decoder are given in this step. Vibration velocity used is 500 mm/s . Time required for the complete scan depends on the number of scan points defined and FFT parameters. In the present analysis, 405 scan points were defined on the composite beam and it took about one hour to complete the scan. After the scan response plots, mode shapes animations are visualized in presentation mode. As shown in Fig. 2.3 component 1 is PSV data extraction system, component 2 contains vibrometer controller and junction box with database management system. Component 3 is scanning laser head which scans all grid point defined on specimen surface. Component 4 is voltage regulator used for controlling the voltage and further component 5 power amplifier is connected. From amplifier component 6 electrodynamic shaker is connected through BNC cables. Component 7 indicates the GFRP specimen clamped on the shaker.

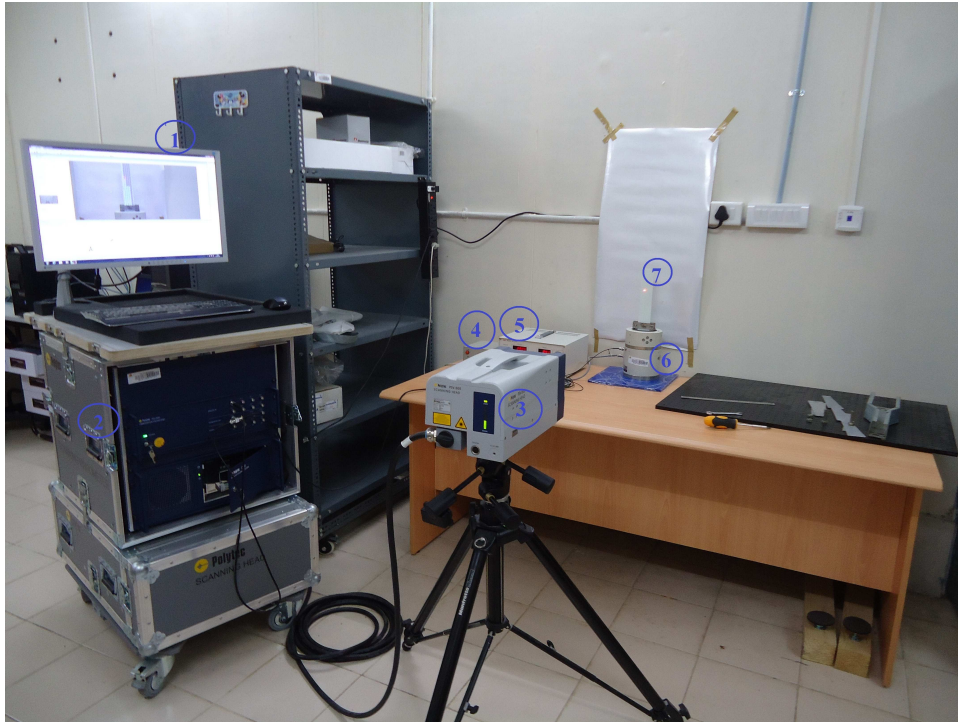


Figure 2.3: Detail Setup of LDV for modal analysis



Figure 2.4: Experimental setup

2.3.1 Specimen Fabrication

Glass fiber reinforced polymer material is chosen for specimen fabrication. For this work initially specimens were fabricated by hand layup technique and later shifted to vacuum assisted resin infusion molding (VARIM) technique for achieving better strength and uniform thickness. Specimen dimensions are 250 mm in length, 50 mm width as considered in Ref. [6] as shown in figure 2.5. Specimens were fabricated with different laminate sequence, namely, uni-directional $[0]_4$, cross-ply $[0/90]_s$, $[0/90]_{2s}$ angle-ply $[45/0/0/45]$ and quasi-isotropic $[45/-45/90/0]_s$. For all four layer laminate configuration total thickness of laminate is 1.2 mm. Teflon tape having 12 mm size is inserted between second and third layer of the laminate to create through-width delamination. In the case of eight layer configuration, total thickness of laminate is 2.4 mm. Delamination is created at two interfaces across the thickness of the laminate. Delamination is introduced between second and third layer i.e. in -45 and 90 and also between sixth and seventh layer in the quasi-isotropic $[45/-45/90/0]_s$ configuration.

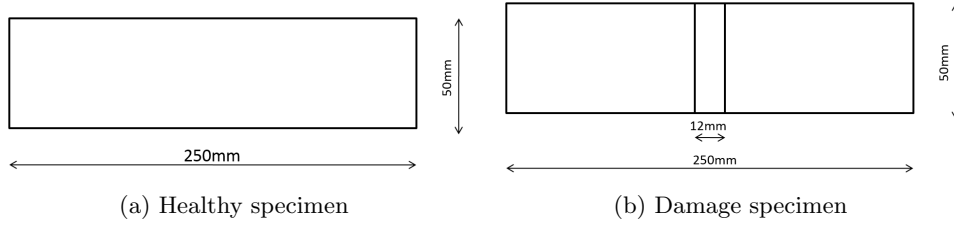


Figure 2.5: Healthy and Damage specimens

Hand Layup Technique

As composite is made of two or more constituents, for preparation of composite laminates first glass fiber material is cut from the Sika(SG930) fiber mat(200gsm) as per required dimension with stacking sequence. Epoxy resin (LY-556) is taken in 1:1 proportion by weight as that of fiber mat and hardener HY-951 (Huntsman) is taken as 1:10 proportion by weight as that of epoxy resin, mixture of both epoxy resin and hardener is used for preparing the casting of the composite laminate using hand layup technique. Teflon tape of 12 mm x 50 mm area of through-width delamination is placed between the middle layers of the composite laminates in centre position during fabrication of specimen casting as shown in Fig. 2.5b. The casted composite laminated sheet was cured for 24 hours. After casting the composite laminates are accurately machined to required dimensions using a milling machine.

Vacuum Assisted Resin Infusion Molding (VARIM)

GFRP specimens are fabricated using vacuum assisted resin infusion molding(VARIM) technique. For fabrication of composite, glass fiber Sika(SG930) fiber-mat material (200gsm) used as fiber and Epoxy resin(CY-230) is taken as 1:1 proportion by weight as that of glass fiber and hardner HY-951(Huntsman) is taken as as 1:10 proportion as that of epoxy resin, mixture of both epoxy resin and hardener is used for preparing the casting of the composite laminate. In this technique initially release agent is applied on prepex sheet surface for releasing purpose. Resin is added between each layer of fiber mat and above which prforated sheet is placed after that peel ply layeris place for

finishing purpose over which breather material is placed for removal of excess resin via suction. This setup is closed on each edge by pasting sealant tape over which a vacuum bag is applied. At one of the end flanges is held which is further connected to a vacuum pump. Figure 2.6 shows specimen fabrication using vacuum assisted resin infusion molding (VARIM). By using this VARIM technique we can produce uniform thickness specimens. Figure 2.7 shows specimens after fabrication by vacuum assisted resin infusion molding.

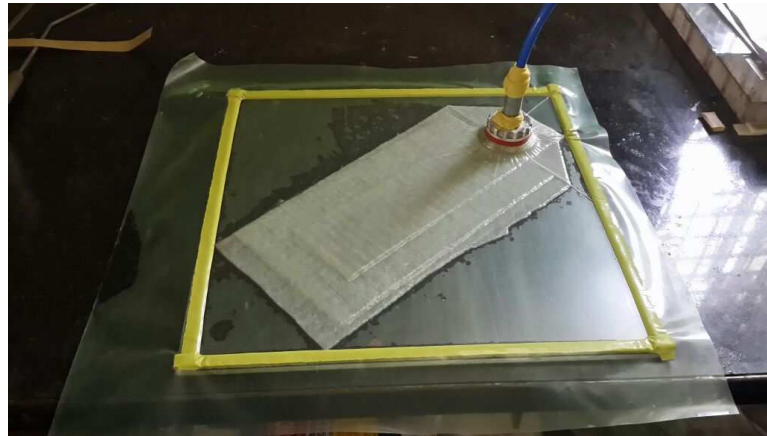


Figure 2.6: Specimen fabrication using VARIM



Figure 2.7: Specimen after fabrication by VARIM

2.3.2 Testing Parameters

In data acquisition parameters are set for controlling excitation signal. Initially in general setting magnitude of excitation is given to avoid unwanted noise which may give faulty results like jerk at the edges of the specimen. Smooth mode shape can be obtained by filtering operation. For this

band pass filter mode is used. In that frequency range is set such as starting frequency should be 1 Hz and ending should be less than half of the sampling frequency. Sampling frequency is a major parameter which depends on bandwidth and number of FFT lines. As sampling frequency will be more which results in lower resolution so that we can get exact fundamental frequency accurately. Magnitude of vibration velocity is set as 500 mm/sec as shown in Fig. 2.8. All testing parameters being used are depicted in Fig. 2.8

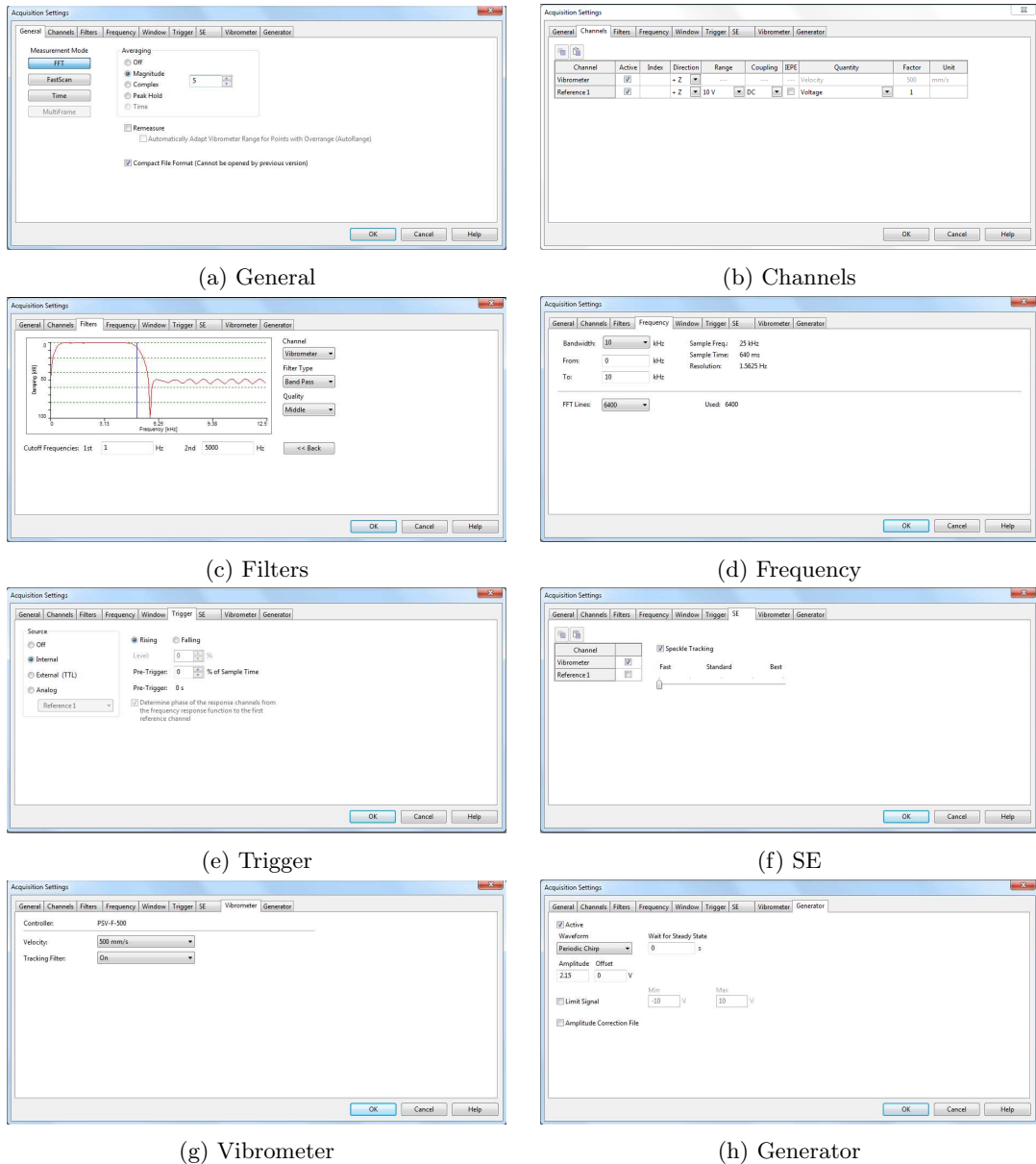


Figure 2.8: Parameter settings for LDV based data acquisition

2.4 Results and Discussions

Due to the presence of delamination in composite beam structure, changes in natural frequency has been observed in case of delaminated composite specimen as compared to healthy one. Since, delamination decreases stiffness so ultimately it affects the natural frequency of the structure. But the effect of delamination on the natural frequencies of composite laminated beam depends on the size and location of the delamination.

2.4.1 Natural Frequencies and FRF

Table 2.1 shows the change in natural frequencies in case of unidirectional $[0]_4$ configuration. There is a change in natural frequency in the case of damage specimen as compared to healthy one. For first and second fundamental mode there is no change in natural frequencies. But for higher modes difference in natural frequencies is notable. Figure 2.9 shows the frequency response function for both healthy and damaged UD GFRP specimen. This frequency change indicates the presence of damage.

| Modes | Healthy, Hz | Delamination, Hz | Change, Hz |
|----------------|-------------|------------------|------------|
| First bending | 18.75 | 18.75 | 0 |
| Second bending | 118.75 | 118.75 | 0 |
| Third bending | 334.38 | 332.96 | 1.42 |
| Fourth bending | 650 | 643.75 | 6.25 |
| Fifth bending | 1075 | 1070.32 | 4.68 |

Table 2.1: Natural frequency for UD GFRP $[0]_4$ specimen obtain using LDV

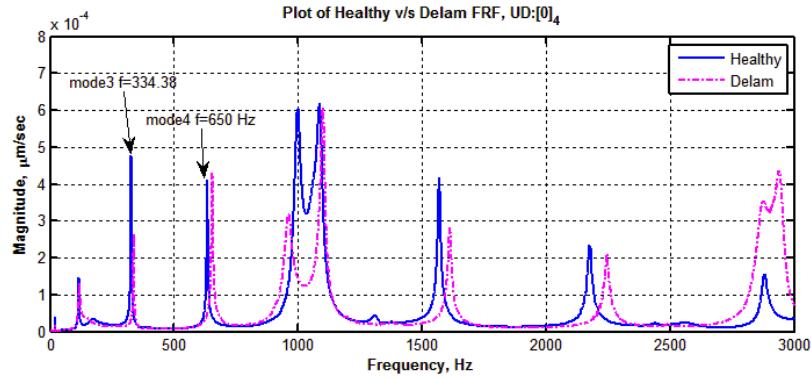


Figure 2.9: Frequency response plot of UD GFRP $[0]_4$ laminate

| Modes | Healthy, Hz | Delamination, Hz | Change, Hz |
|----------------|-------------|------------------|------------|
| First bending | 17.2 | 17.2 | 0 |
| Second bending | 109.38 | 109.38 | 0 |
| Third bending | 303.12 | 295 | 8.12 |
| Fourth bending | 587.5 | 584.38 | 3.12 |
| Fifth bending | 1000 | 990.63 | 9.37 |

Table 2.2: Natural frequency for cross-ply GFRP $[0/90]_s$ obtain using LDV

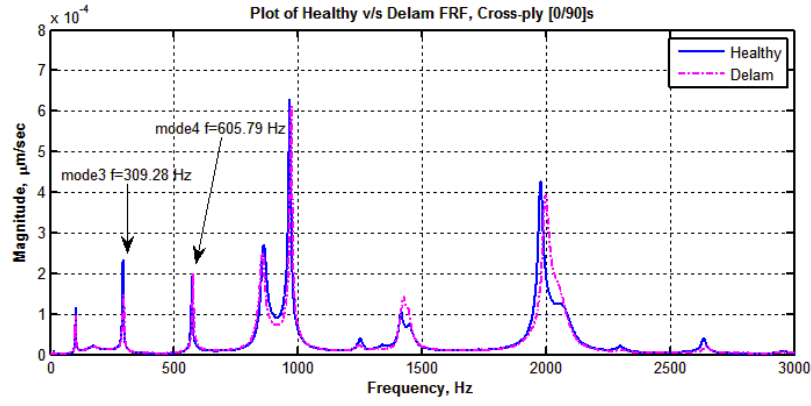


Figure 2.10: Frequency response plot of cross-ply GFRP $[0/90]_s$ laminate

| Modes | Healthy, Hz | Delamination, Hz | Change, Hz |
|----------------|-------------|------------------|------------|
| First bending | 11.3 | 11.3 | 0 |
| Second bending | 71.3 | 68.8 | 2.5 |
| Third bending | 201.3 | 201.3 | 0 |
| Fourth bending | 400 | 392.5 | 7.5 |
| Fifth bending | 656.3 | 653.8 | 2.5 |

Table 2.3: Natural frequency for angle-ply GFRP $[45/0/0/45]$ obtain using LDV

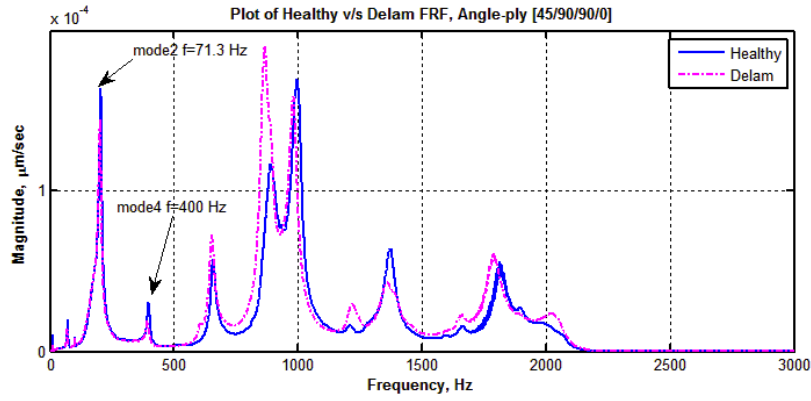


Figure 2.11: Frequency response plot of angle-ply GFRP $[45/0/0/45]$ laminate

| Modes | Healthy, Hz | Delamination, Hz | Change, Hz |
|----------------|-------------|------------------|------------|
| First bending | 37.5 | 37.5 | 0 |
| Second bending | 275 | 275 | 0 |
| Third bending | 687.5 | 675 | 12.5 |
| Fourth bending | 1450 | 1425 | 25 |
| Fifth bending | 2362.5 | 2350 | 12.5 |

Table 2.4: Natural frequency for cross-ply GFRP $[0/90]_{2s}$ obtain using LDV

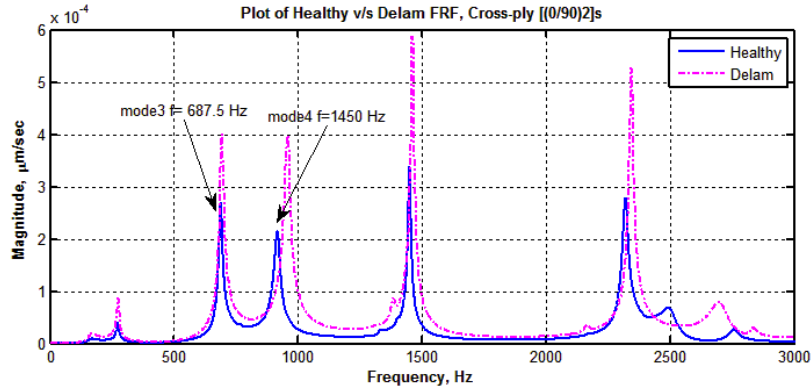


Figure 2.12: Frequency response plot of cross-ply GFRP $[0/90]_{2s}$ laminate

| Modes | Healthy, Hz | Delamination, Hz | Change, Hz |
|----------------|-------------|------------------|------------|
| First bending | 22.5 | 21.9 | 0.6 |
| Second bending | 142.5 | 140.62 | 1.88 |
| Third bending | 400 | 398.4 | 1.6 |
| Fourth bending | 801.25 | 796.875 | 4.38 |
| Fifth bending | 2362.5 | 2350 | 12.5 |

Table 2.5: Natural frequency for quasi, $[45/-45/90/0]_s$ GFRP specimen obtain using LDV

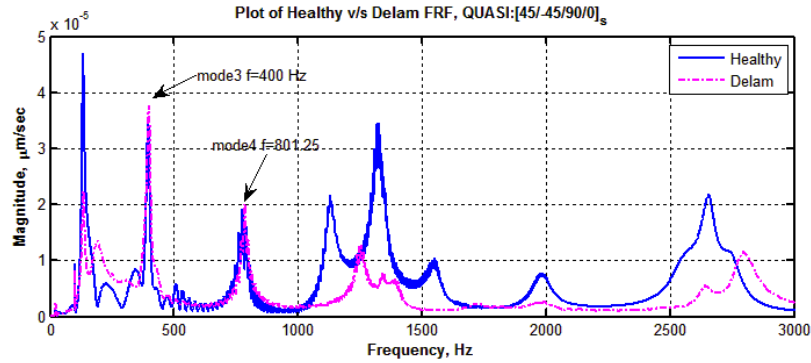


Figure 2.13: Frequency response plot of quasi-isotropic GFRP $[45/-45/90/0]_s$ laminate

Similarly, in Table 2.2 shift in natural frequency is observed in delamination case of delamination specimen as compared to healthy one for cross-ply $[0/90]_s$ configuration. Also the FRF plot as shown in Fig. 2.10 indicates frequency change for higher modes especially for third and fourth mode. As the trend shown in Fig. 2.10 shows peaks at certain frequency which give the magnitude of instantaneous velocity of vibrating specimen obtained by Fast Fourier Transform (FFT) analyser which is inbuilt in the LDV equipment that converts the time signal into frequency domain using FFT analyser directly gives the FRF plot of magnitude of excitation velocity in micrometer per seconds versus frequency in Hz. For angle-ply $[45/0/0/45]$ configuration natural frequencies are shown in Table 2.3

where third frequency is dominant as it is showing higher difference in natural frequencies and FRF plot is in Fig. 2.11 where shift in natural frequency is indicated by an arrow. For cross-ply $[0/90]_{2s}$ change in natural frequencies are presented in Table 2.4 and higher modes shift is predominant. Also FRF plot represents the change in natural frequency as shown in figure 2.12, where third and fourth frequency are indicated by an arrow. For quasi-isotropic laminate change in natural frequencies is shown in Table 2.5 where shift in all natural frequencies is observed and most dominating is fifth one. FRF plot is presented in Fig. 2.13.

This concludes that change in natural frequencies is the indication of presence of damage. But only change in natural frequency and FRF plots are not sufficient for getting damage information of structure. For locating delamination another subsequent parameter required is mode shape.

2.4.2 Experimental Mode Shapes

Mode shape are widely used as an alternative to locate the damage as it is subsequent parameter which carries the information of damage location. So, mode shapes information is required for locating the delamination. It is essential to get smooth mode shape from which curvature information is derived numerically by numerical differentiation process. Figure 2.14 shows comparison of healthy versus delamination mode shapes obtained from LDV experiment for unidirectional $[0]_4$ laminate where mode shapes obtained for delamination case are nearly matching with healthy one. Similarly, figure 2.15 shows comparison of healthy and delamination mode shapes for cross-ply $[0/90]_s$ lamiate where first two modes are for delamiantion case are nearly matching with healthy one. But for third mode for delamiantion case mix mode coupling is happening as shown in Fig. 2.15f beacuae of clamping condition. As shown in figure 2.16 comparison of healthy and delamination mode shapes for angle-ply $[45/0/0/45]$ laminate are nearly same. In case angle-ply $[45/0/0/45]$ laminate bending-extension coupling is happening in behaviour of mode shapes because all bending stiffness for this laminate are positive definite. Figure 2.17 shows mode shape for cross-ply $[0/90]_{2s}$ laminate where where one can observe that for mode shapes for healthy and delaminated beams compare qualitatively. But nature of the fifth mode shape is not purely bending as composite material is ortotropic material and this cross-ply $[0/90]_{2s}$ laminate is made of hand layup technique. So some sort of variation may occurs in the thickness of laminate which may affects in bending-extension type of coupling for higher modes. Figure 2.18 shows the comparison of mode shapes of healthy versus delamination beam for $[45/-45/90/0]_s$ laminate. From this one can observe that mode shapes delaminated beams compare qualitatively as that of healthy one.

The modal data is exported in ASCII format from PSV 9.0 acquisition software. Further it is imported in MATLAB for getting mode shapes. The ASCII format stores the information about x, y and z position and instantaneous velocity in out of plane direction of the scan grid points defined on specimen which are scanned by laser head. These information is enough for plotting the mode shape using MATLAB. To locate the delamination curvature mode is essential. Thus, curvature mode shape is obtained by numerical differentiation of mode shape. Damage location is found out by applying various damage detection algorithms which is discussed in next chapter.

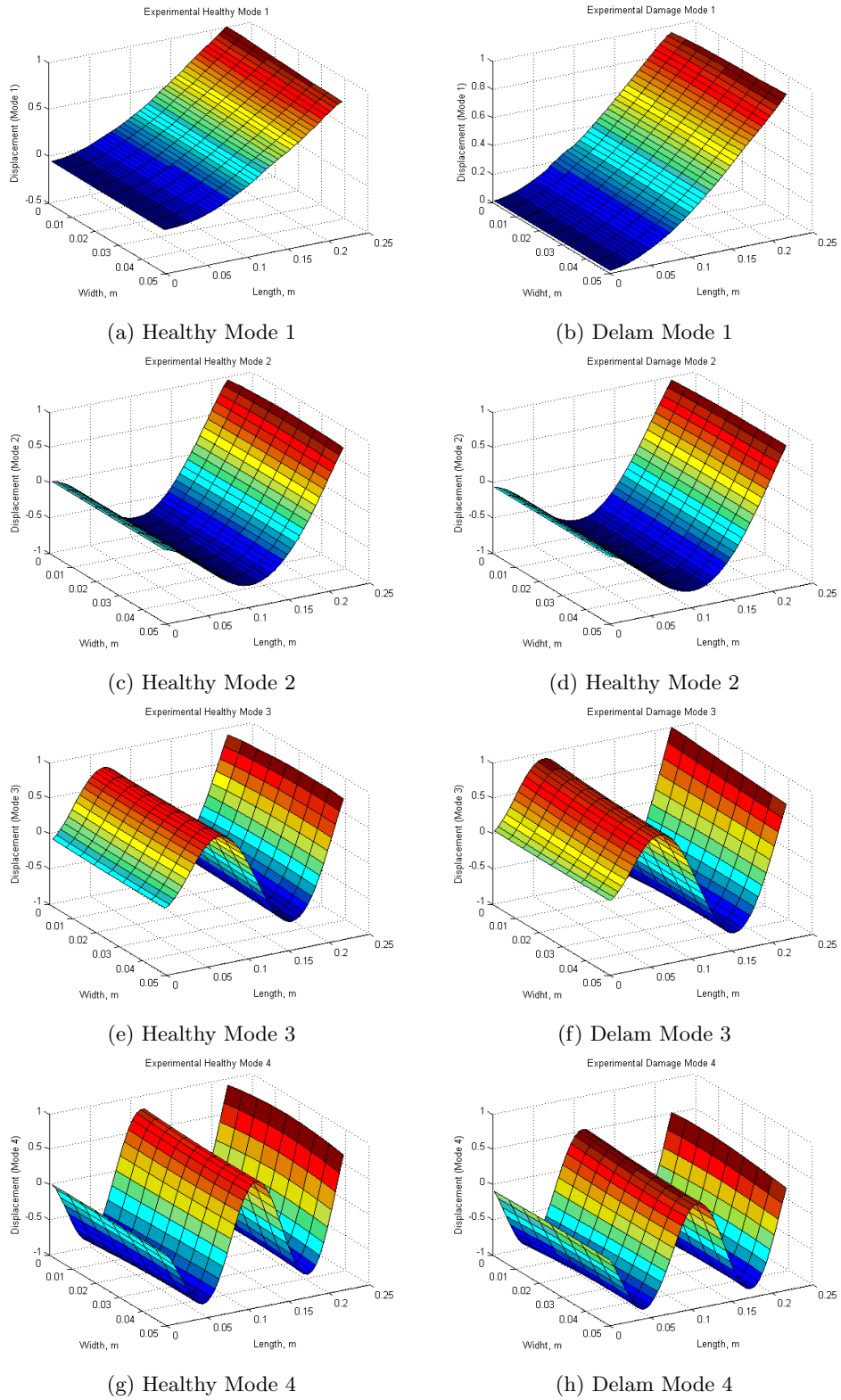


Figure 2.14: Displacement mode shapes for UD GFRP $[0]_4$ obtained from LDV

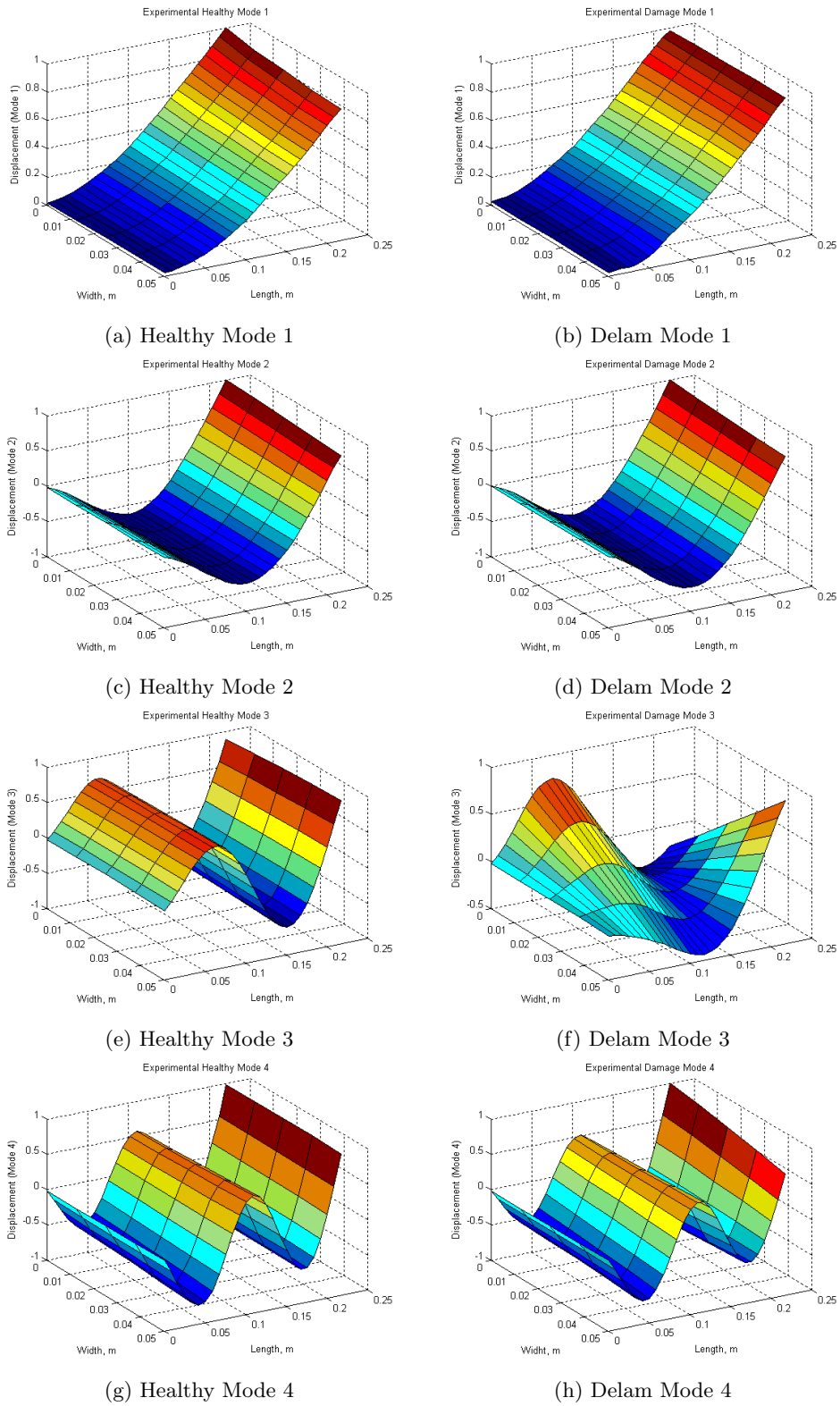


Figure 2.15: Displacement mode shapes for cross-ply GFRP $[0/90]_s$ obtained from LDV

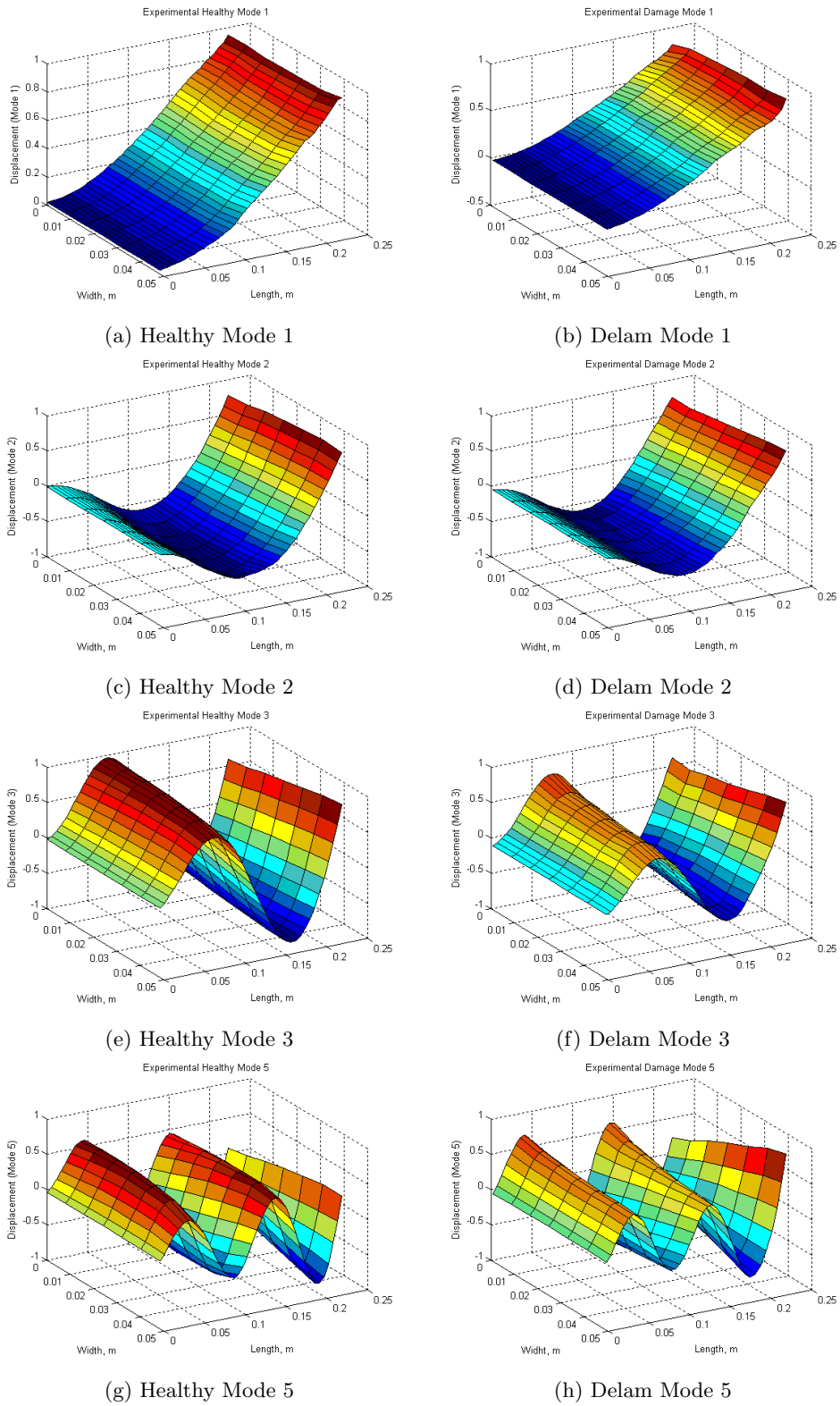


Figure 2.16: Displacement mode shapes for angle-ply GFRP [45/0/0/45] obtained from LDV

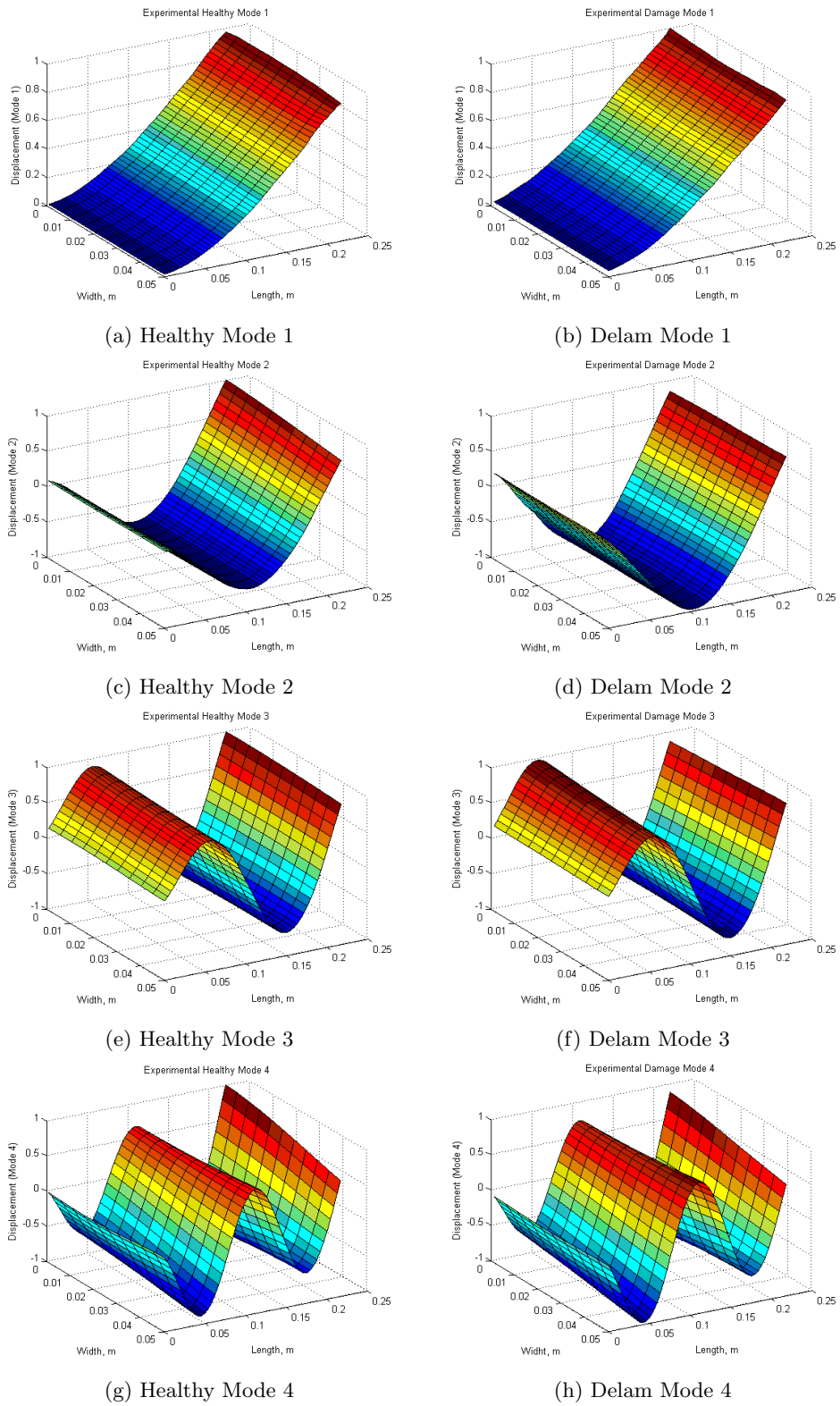


Figure 2.17: Displacement mode shapes for cross-ply GFRP $[0/90]_{2s}$ obtained from LDV

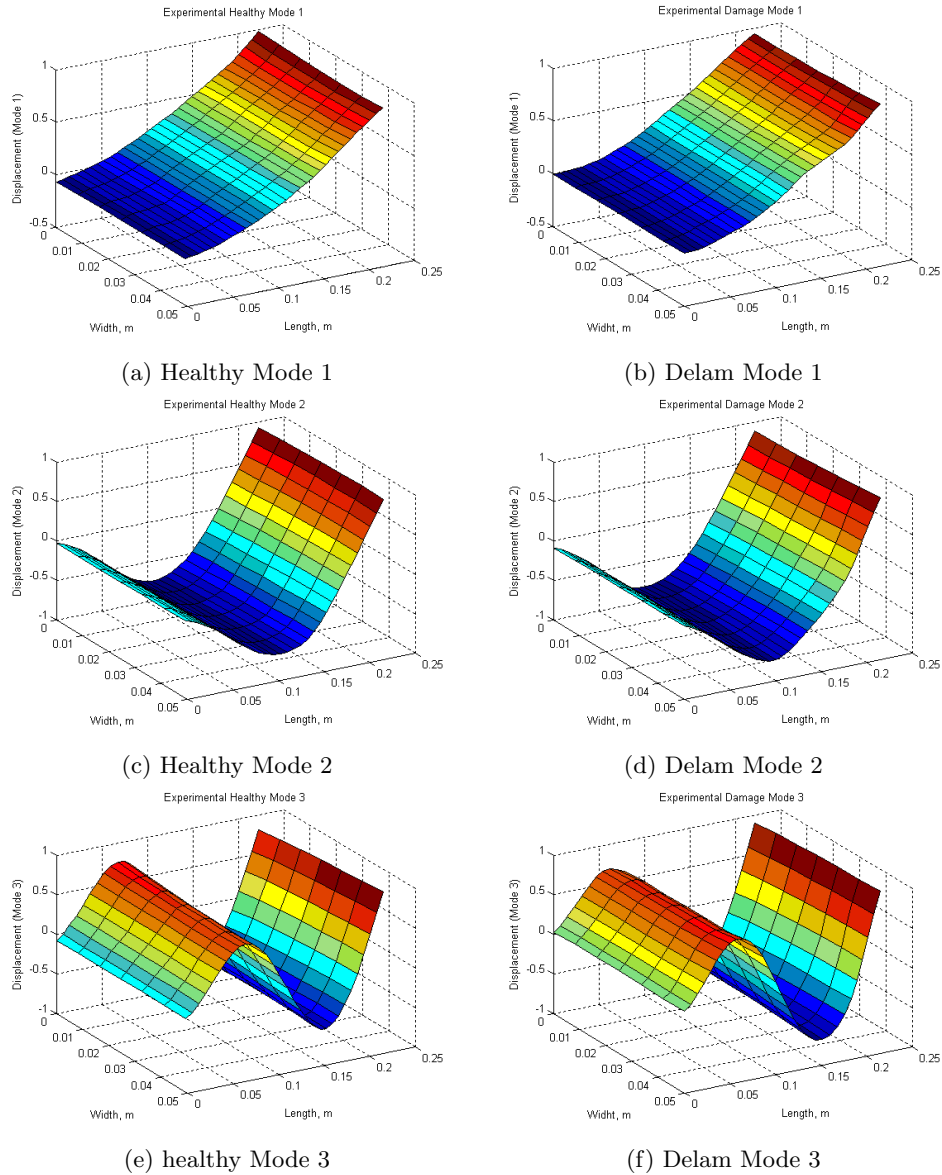


Figure 2.18: Displacement mode shapes for quasi-isotropic GFRP $[45/-45/90/0]_s$ obtained from LDV

2.5 Closure

Experimentally, change in natural frequencies are observed in delamination beam as compared to healthy one. From FRF plot frequency change trend can be observed. Shift in natural frequencies and mode shapes are giving information about the presence of damage. Here, at higher mode shapes frequency shifts are predominant. Mode shapes for healthy and delamination specimen are compare qualitatively for different configuration.

Chapter 3

Finite Element Analysis and Modal Study

3.1 Introduction

In this chapter finite element (FE) modeling of through width delamination in composite beams was carried out to study their effect on the modal characteristics of the beam. The modal analysis of composite beams was done using commercial ANSYS finite element solver. Both shell and solid FE elements were used to model the composite beam and contact elements were used to model the delamination in the beam. Glass fiber reinforced composite specimens of different layup configuration with and without delamination were studied and their modal characteristics compared to get information regarding the detection, location and quantification of damage in the structure.

3.2 Finite element modeling

For the numerical study, cantilever composite beam specimens of dimensions, 220 mm in length and 50 mm in width were chosen [6]. Delamination is modeled at midspan of the beam having a dimensions of 12 mm length and 50 mm width. The composite beams were modeled using eight noded brick element SOLID185 available in ANSYS software. Finite element mesh density of 100×20 was chosen for the study for each lamina based on convergence study. The Block-Lanczos solver was used to perform the modal analysis and extract the natural frequencies and the mode shapes of the composite beams.

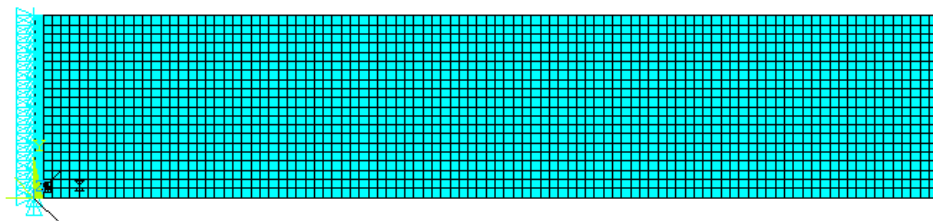


Figure 3.1: Element plot

3.3 Delamination Modeling

In this study, different laminate sequence, namely, uni-directional $[0]_4$, cross-ply $[0/90]_s$, $[0/90]_{2s}$ angle-ply $[45/0/0/45]$ and quasi-isotropic $[45/-45/90/0]_s$ were studied. For all four layer laminate configuration, delamination is modeled between second and third layer of the laminate. In the case of eight layer configuration, delamination is modeled at two interfaces across the thickness of the laminate. Delamination is introduced between second and third layer i.e. in -45 and 90 and between sixth and seventh layer in the composite laminate. The delaminated beam is modeled as two sub-laminates, separated along the interface at which the delamination is located. The nodes associated along the interface of undelaminated region are merged together while nodes in the interface of delaminated area are separated. To avoid the separation of these two sub-laminates for representation of delamination, contact elements (TARGE170/CONTAC174) are created using contact manager setting. Contact plot is shown in Fig. 3.2. Subsequently, multi-point constraint (MPC) algorithm is used to create the contact between the delaminated surfaces as shown in Fig. 3.3.

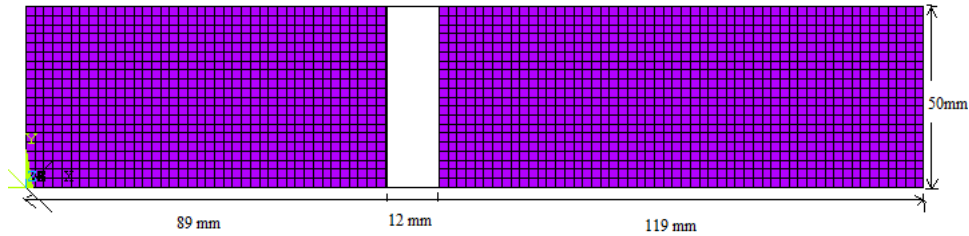


Figure 3.2: Delamination contact plot

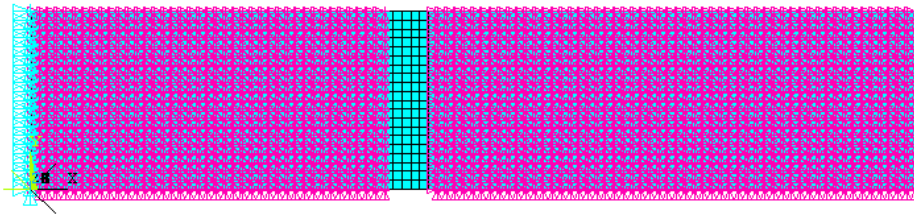


Figure 3.3: Delamination using MPC Algorithm

3.4 Results and Discussions

3.4.1 Validation of FE results with analytical results

To start with, the modal analysis results obtained used FE model of delaminated composite beam were compared with analytical model results given by CN Della and Shen [17, 22]. The composite

laminate was made of T300/934 graphite/epoxy and the material properties are given in Table 3.1. The dimensions of composite beam are $127 \times 12.7 \times 1.016 \text{ mm}^3$ and the stacking sequence is chosen to be $[0/90]_{2s}$. The delaminations were modelled at midspan of the beam and their lengths were chosen to be 25.4, 50.8, 76.2, and 101.6 mm. The location of delamination along the thickness direction is shown in Fig. 3.4 [17]. Natural frequency results of the delaminated composite beam obtained using FE and analytical solution are shown in Table 3.2 and they match quite well. Thus, from this study we conclude that FE modelling validates the modal analysis results as given in literature and we use them to study the delamination in GFRP laminates.

| GFRP Composite Laminate Properties | Values [17, 22] |
|-------------------------------------|-----------------|
| E_{11} (GPa) | 134 |
| E_{22} (GPa) | 10.3 |
| E_{33} (GPa) | 10.3 |
| ν_{12} | 0.33 |
| ν_{23} | 0.48 |
| ν_{13} | 0.33 |
| G_{12} (GPa) | 5 |
| G_{23} (GPa) | 3.59 |
| G_{13} (GPa) | 3.48 |
| Density, ρ (Kg/m^3) | 1480 |

Table 3.1: Material properties of GFRP Laminates

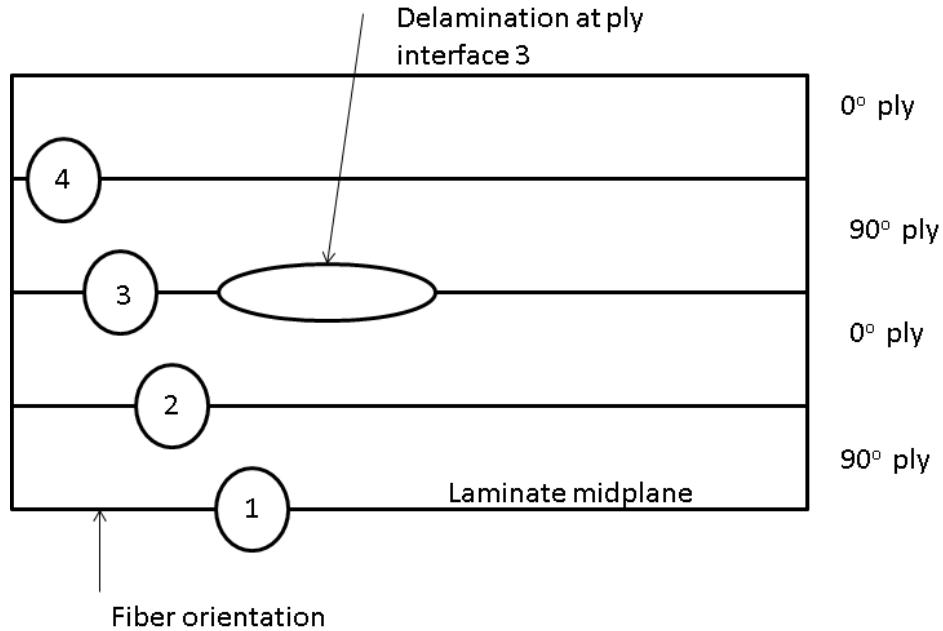


Figure 3.4: Thicknesswise location of Delamination

| Fundamental natural frequency, Hz | | |
|-----------------------------------|------------------|----------|
| Delamination length | Analytical model | FE Model |
| Healthy | 82.042 | 81.894 |
| 25.4 mm | 80.133 | 81.08 |
| 50.8 mm | 75.285 | 76.301 |
| 76.2 mm | 66.936 | 67.066 |
| 101.6 mm | 57.239 | 56.419 |

Table 3.2: Fundamental natural frequencies delamination along interface 1

3.4.2 Validation of FE results with Experimental results

FE modelling results of GFRP laminates are validated with results obtained from experimental analysis as discussed in previous chapter. In FE modelling glass fiber reinforced polymer material properties are used as shown in Table 3.3 and material properties are obtained by characterization test. FE models are created as per required configuration with different stacking sequence. Delamination models are created for through-width delamination of standard size 12 mm used as discussed in the previous section.

| GFRP Composite Laminate Properties | DIC values(Average) |
|------------------------------------|---------------------|
| E_{11} (GPa) | 26.31 |
| E_{22} (GPa) | 9.68 |
| E_{33} (GPa) | 9.68 |
| ν_{12} | 0.29 |
| ν_{23} | 0.37 |
| ν_{13} | 0.29 |
| G_{12} (GPa) | 2.48 |
| G_{23} (GPa) | 3.59 |
| G_{13} (GPa) | 2.48 |
| Density, ρ (Kg/m^3) | 1728 |

Table 3.3: Material properties of UD GFRP Laminates obtained using DIC Technique

| Modes | Natural Frequency, Hz | | | |
|--------------|-----------------------|--------|---------|---------|
| | Healthy | | Damage | |
| | FEA | LDV | FEA | LDV |
| First mode | 18.997 | 18.75 | 18.995 | 18.75 |
| Second mode | 118.99 | 118.96 | 118.75 | 118.75 |
| Third mode | 333 | 332.96 | 332.82 | 332.82 |
| Fourth mode | 652.12 | 651.04 | 650 | 646.875 |
| Fifth mode | 1077.1 | 1075.2 | 1075 | 1070.32 |
| Sixth mode | 1607.3 | 1596.2 | 1607.82 | 1600 |
| Seventh mode | 2240.2 | 2238.8 | 2240.62 | 2220.32 |

Table 3.4: Comparison Natural frequencies for GFRP UD $[0]_4$ using FEA and LDV

| Modes | Natural Frequency, Hz | | | |
|--------------|-----------------------|---------|--------|---------|
| | Healthy | | Damage | |
| | FEA | LDV | FEA | LDV |
| First mode | 17.64 | 17.2 | 17.63 | 17.2 |
| Second mode | 110.5 | 109.38 | 110.47 | 109.38 |
| Third mode | 309.28 | 303.12 | 308.94 | 303.12 |
| Fourth mode | 605.79 | 587.5 | 604.87 | 584.38 |
| Fifth mode | 1000.8 | 1000 | 999.21 | 990.63 |
| Sixth mode | 1494 | 1457.82 | 1484.8 | 1454.68 |
| Seventh mode | 2083.9 | 2025 | 2082.6 | 2012.5 |

Table 3.5: Comparison Natural frequencies for GFRP cross-ply $[0/90]_s$ using FEA and LDV

| Modes | Natural Frequency, Hz | | | |
|-------------|-----------------------|-------|--------|-------|
| | Healthy | | Damage | |
| | FEA | LDV | FEA | LDV |
| First mode | 13.96 | 11.3 | 13.95 | 11.3 |
| Second mode | 87.08 | 71.3 | 87.04 | 68.8 |
| Third mode | 244.01 | 201.3 | 243.82 | 201.3 |
| Fourth mode | 478.52 | 400 | 477.95 | 392.5 |
| Fifth mode | 791.12 | 656.3 | 790.15 | 653.8 |
| Sixth mode | 1179.74 | 991.3 | 1175.8 | 981.3 |

Table 3.6: Comparison Natural frequencies for GFRP angle-ply $[45/0/0/45]$ using FEA and LDV

| Modes | Natural Frequency, Hz | | | |
|-------------|-----------------------|--------|--------|------|
| | Healthy | | Damage | |
| | FEA | LDV | FEA | LDV |
| First mode | 38.745 | 37.5 | 38.738 | 37.5 |
| Second mode | 242.22 | 275 | 242.15 | 275 |
| Third mode | 676.19 | 687.5 | 674.54 | 675 |
| Fourth mode | 1319.8 | 1450 | 1315.4 | 1425 |
| Fifth mode | 2169.4 | 2362.5 | 2161.8 | 2350 |

Table 3.7: Comparison Natural frequencies for GFRP cross-ply $[0/90]_{2s}$ using FEA and LDV

| Modes | Natural Frequency, Hz | | | |
|-------------|-----------------------|--------|--------|---------|
| | Healthy | | Damage | |
| | FEA | LDV | FEA | LDV |
| First mode | 26.290 | 22.5 | 26.276 | 21.9 |
| Second mode | 164.27 | 142.5 | 164.10 | 140.62 |
| Third mode | 460 | 400 | 458.89 | 398.4 |
| Fourth mode | 902.26 | 801.25 | 899.09 | 796.875 |
| Fifth mode | 1492.1 | 1315.6 | 1486.7 | 1315.6 |

Table 3.8: Comparison Natural frequencies for GFRP quasi $[45/-45/90/0]_s$ using FEA and LDV

Shift in natural frequency is observed for all configurations, for unidirectional $[0]_4$ shift in natural frequency is presented in Table 3.4 in case of damage specimen from both FEA and LDV. Shift in natural frequency is not severe for fundamental frequency but for higher modes difference in natural frequencies is dominant this change in natural frequencies indicates the presence of damage. For other configuration such as cross-ply $[0/90]_s$, $[0/90]_{2s}$, angle-ply $[45/0/0/45]$ and quasi-isotropic $[45/-45/90/0]_s$ difference is observed for higher natural frequencies as represented in above tables. Table 3.7 shows change in natural frequencies for $[0/90]_{2s}$ laminate. It is noticeable that for first fundamental natural frequency obtain from LDV is compare qualitatively. Eventually experimental natural frequencies shows distinct change as compared with natural frequencies obtained from FEA. This is happening due to beacause of laminate thickness as it is cross-ply $[0/90]_{2s}$ laminate and fabricated using hand layup technique, so thickness variation can not be controlled by this technique. The change in natural frequencies for quasi-isotropic $[45/-45/90/0]$ laminate are shown in Table 3.8 which indicates that natural frequency is dependent on laminate sequence as well as laminate thickness. For both cross-ply $[0/90]_{2s}$ and quasi-isotropic $[45/-45/90/0]_s$ laminates one can notice distinct difference in natural frequency. This concludes that change in natural frequencies is the indication of presence of damage. Since, modal parameters are the function of structural properties such as stiffness, mass and modal damping etc. Therefore, difference in natural frequencies ultimately affects on stiffness of the composite beam and reduces its stiffness. The shift in natural frequency is giving the information of presence of damage which is not sufficient to locate the damage. Subsequently, another parameter mode shape is needed for locating the damage present in composite beam. Since, it is carrying damage information of the composite beam. So, mode shapes are widely used as an alternative for identification of location of damage. Fig. 3.5 shows comparison of delamination modes shapes obtained from FEA and LDV where all modes are qualitatively compared. For unidirectional $[0]_4$ and cross-ply $[0/90]_s$ laminate all mode shapes obtained are bending in nature as it is made of orthotropic material. For other configurations mode shapes are compare qualitatively. For cross-ply $[0/90]_s$ laminate modes shapes are shown in Figure 3.6 in case of delaminated composite beam. As in case of cross-ply laminate, for higher mode shapes mix-mode coupling is happening particularly during experiments as shown in Fig. 3.6f due to beacause of clamping condition. For angle-ply $[45/0/0/45]$ laminate all modes shapes are compare qualitatively which causes bending-extention coupling. Since, for angle-ply $[45/0/0/45]$ laminate all bending (flexural) stiffness are positive. Experimentally as well as numerically modes shapes are having bending with twisting behavior as shown in Fig. 3.7. For cross-ply $[0/90]_{2s}$ laminate delamination is present between fourth and fifth layer and for quasi-isotropic $[45/-45/90/0]_s$ lamianate delamination is present in two interfaces as discussed in previous section and it is 89 mm apart from fix end as shown in Fig.3.2. Figure 3.7 shows comparison of mode shapes for FEA and LDV. For cross-ply stacking sequence bending stiffness, D_{16} is negative while D_{26} is positive. In case of quasi-isotropic laminate all bending stiffnesses are positive. It represents that mode shapes obtained from LDV are in compare qualitatively with FEA. The damage information obtained from LDV results should be smooth because for locating the damage numerical differentiation of mode shape is required. Sometimes we can get jerks near clamped edge or along free edge to avoid these jerk which reflects in the wrong results smoothing is required.

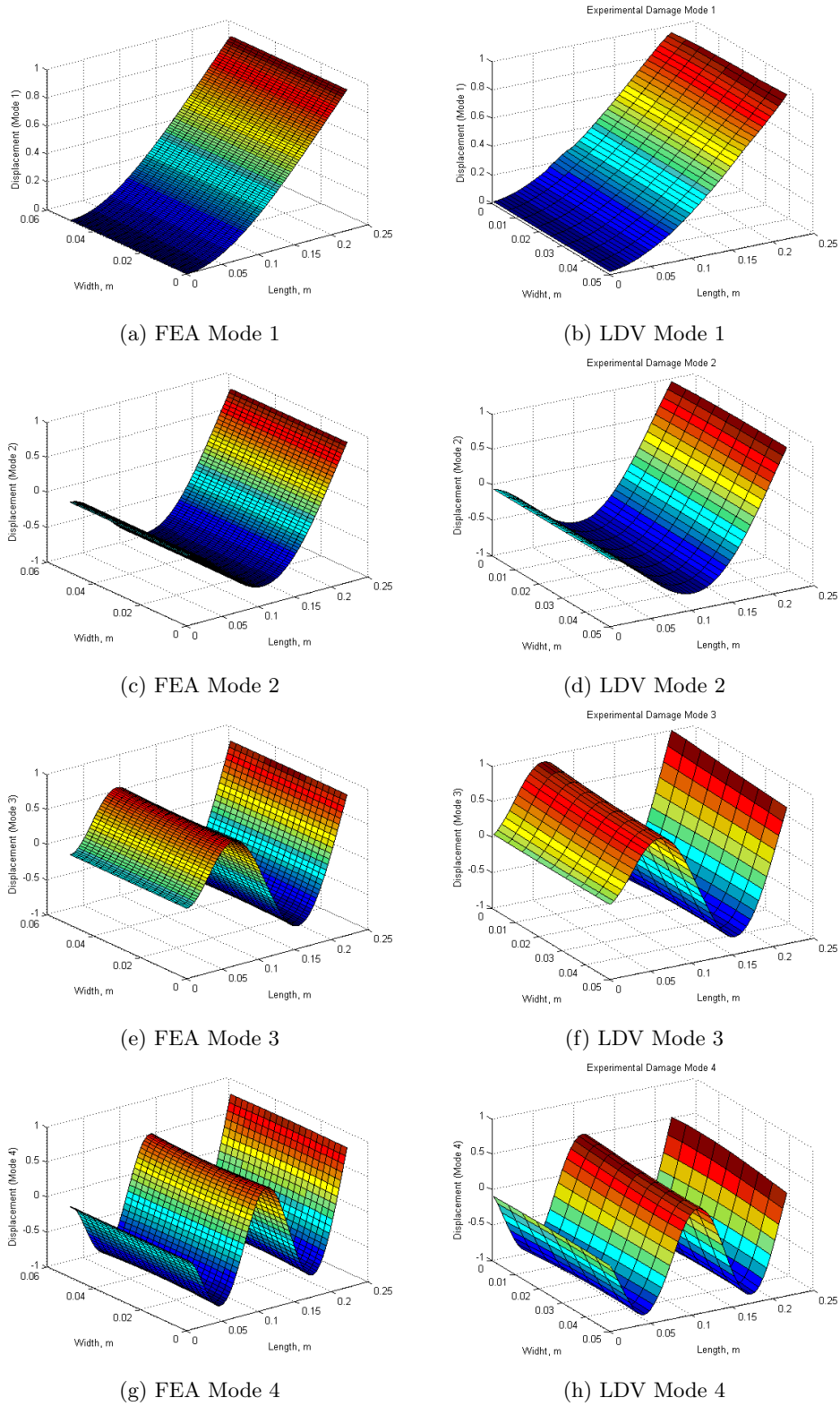


Figure 3.5: Displacement Modeshapes for GFRP unidirectional $[0]_4$ laminate using FEA and LDV

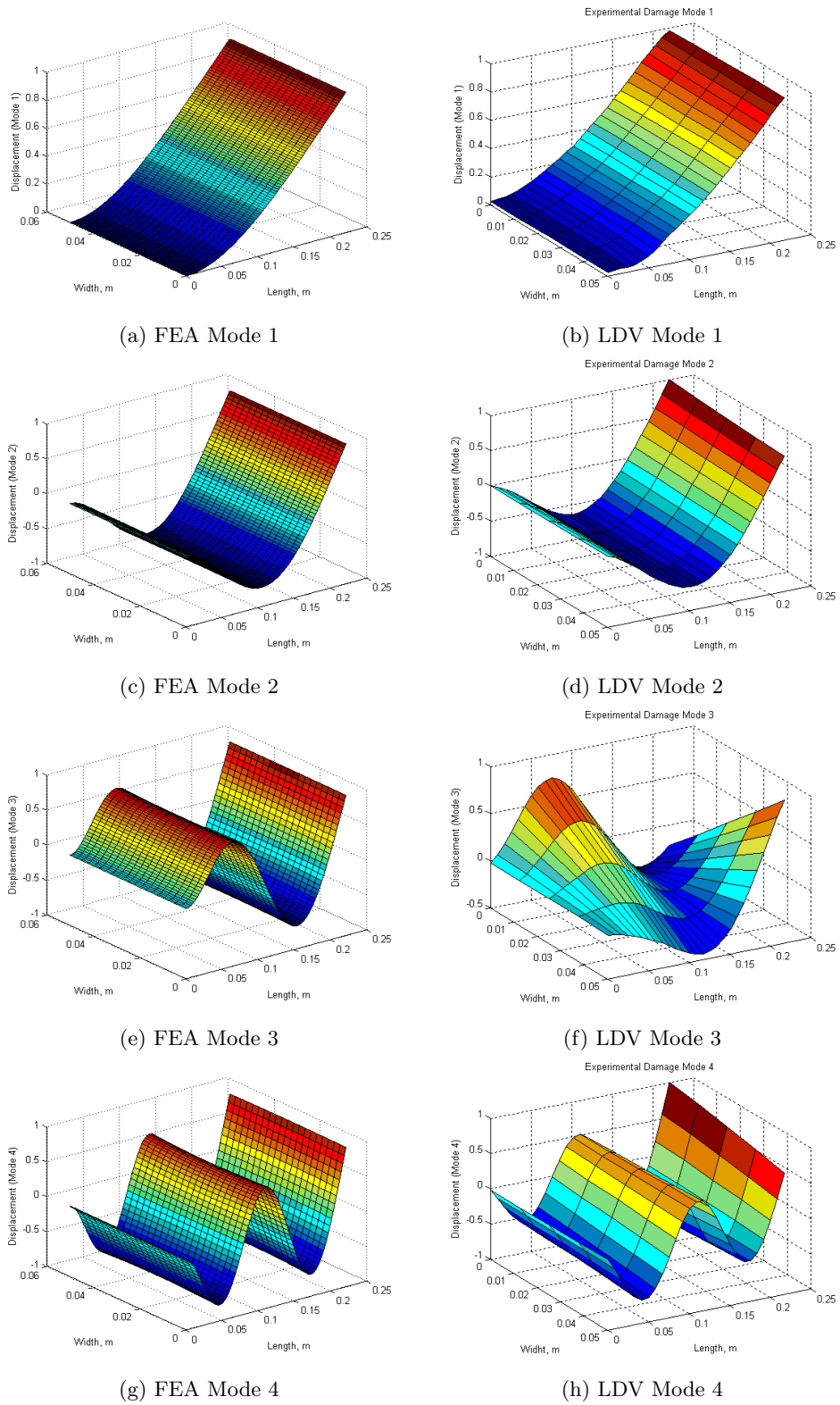


Figure 3.6: Displacement Modeshapes for GFRP cross-ply $[0/90]_s$ laminate using FEA and LDV

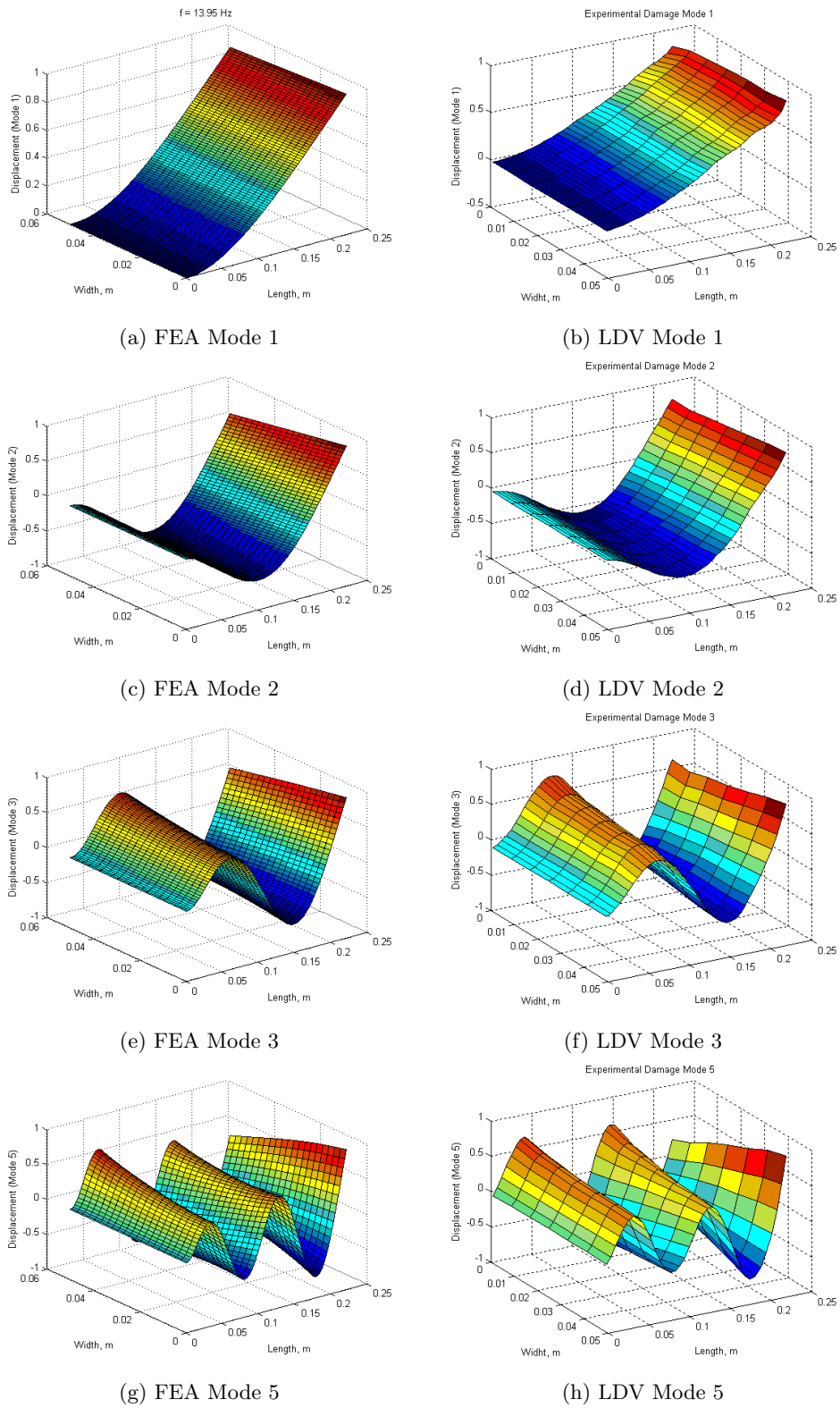


Figure 3.7: Displacement Modeshapes for GFRP angle-ply [45/0/0/45] laminate using FEA and LDV

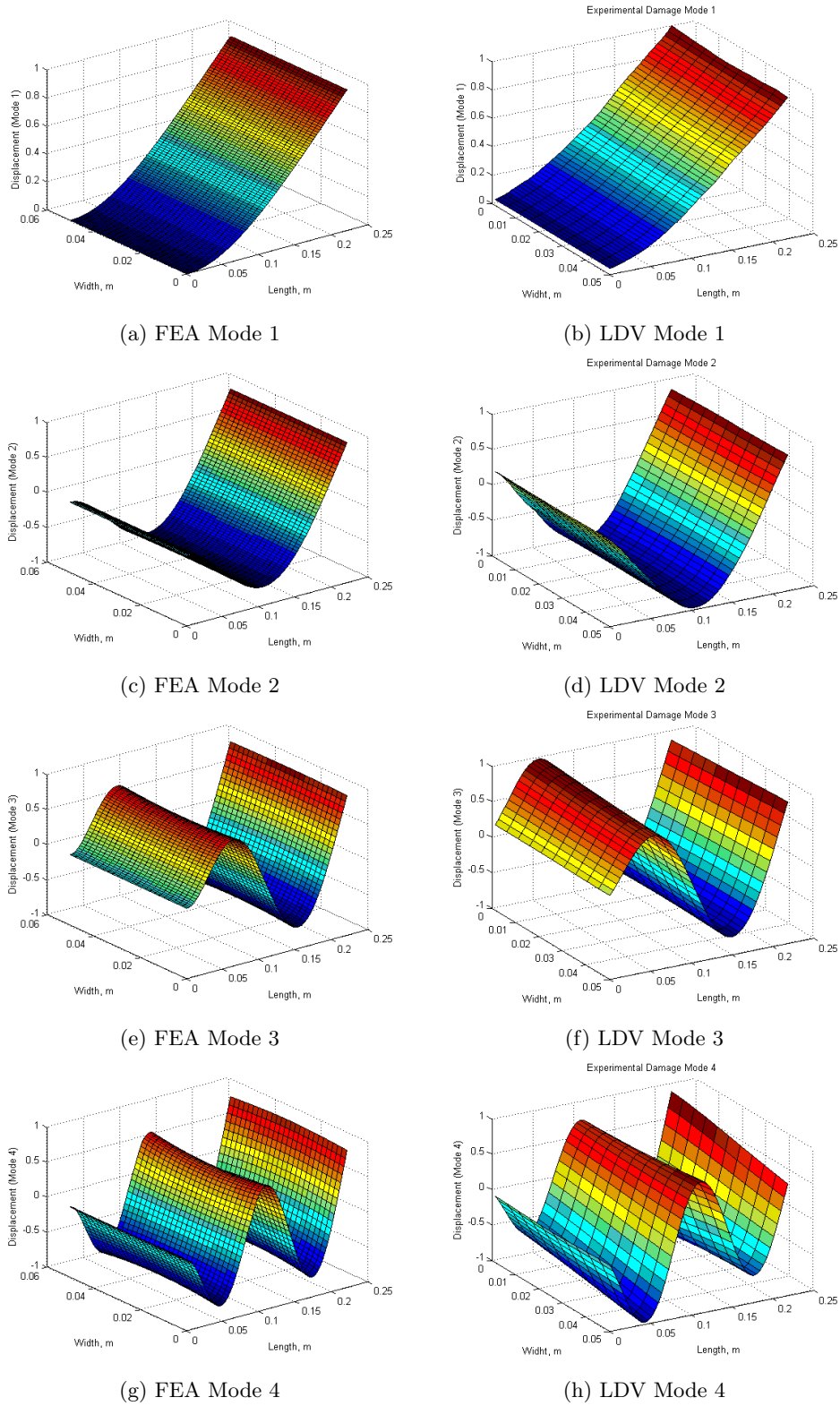


Figure 3.8: Displacement Modeshapes for GFRP cross-ply $[0/90]_{2s}$ laminate using FEA and LDV

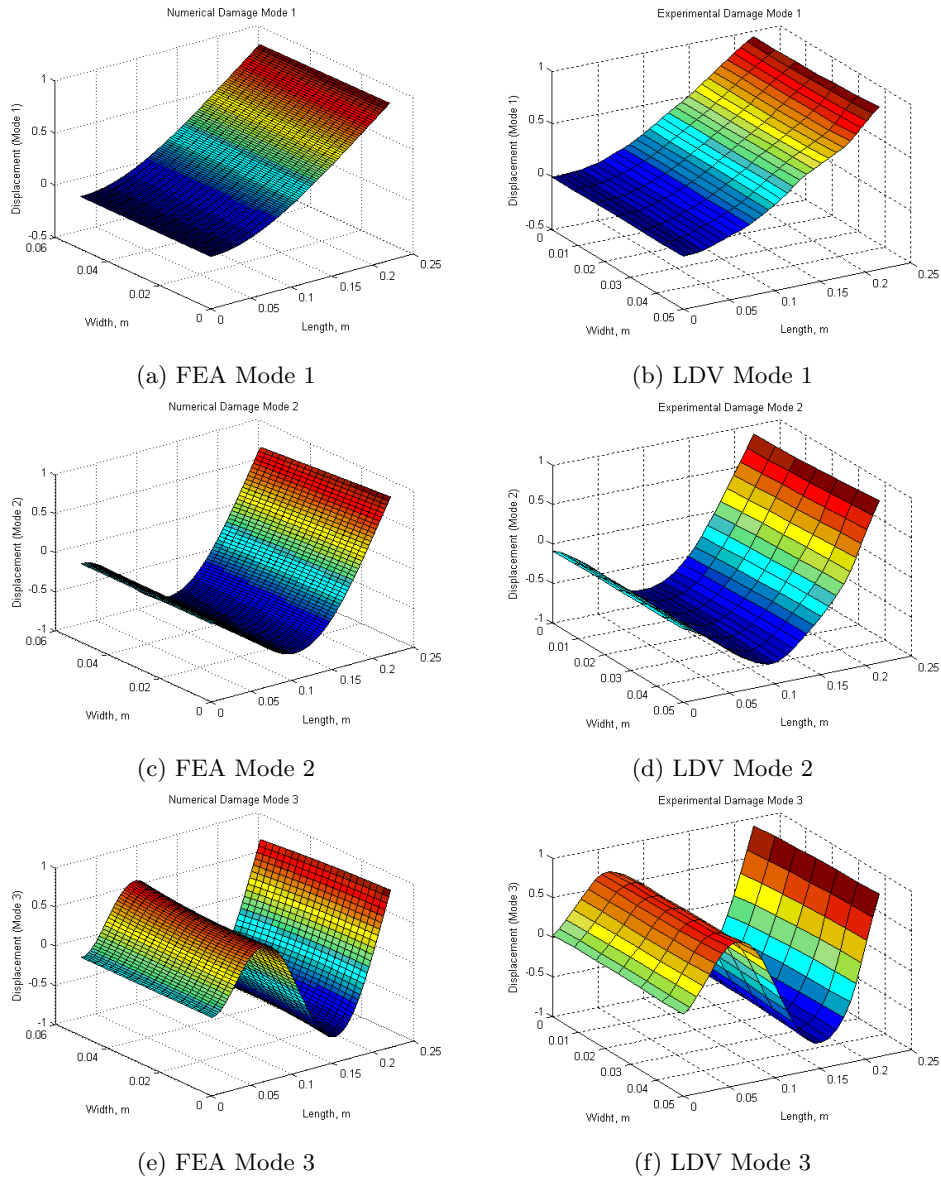


Figure 3.9: Displacement Modeshapes for GFRP quasi-isotropic $[45/ - 45/90/0]_s$ laminate using FEA and LDV

From modal data obtained from numerical FE results, curvature mode shapes are obtained by numerical differentiation of mode shapes to represent the location of delamination. Curvature mode 2 for quasi laminate is shown in Fig. 3.10 where delamination location is presented by an arrow. Curvature mode 3 for quasi-isotropic $[45/ - 45/90/0]$ is plotted delaminated over the healthy as shown in Figure 3.11 where sort of jump is presented in between 0.089 m to 0.101 m which indicates the presence of damage and represented by an arrow. Similarly, curvature mode 4 for the same configuration is shown in Fig. 3.12 where same trend is shown by dotted line represents presence of delamination. From the above curvature plots it is concludes that curvature mode shape plays an important role for locating damage present in the structure. Subsequently, damage detection algorithms are applied to the curvature mode shape data to exactly locate the delamination.

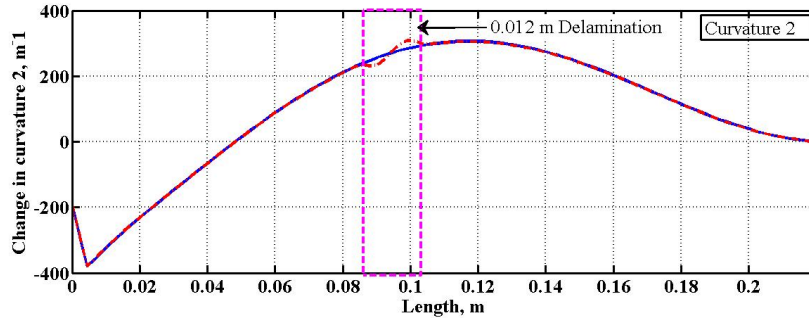


Figure 3.10: Quasi Curvature 2

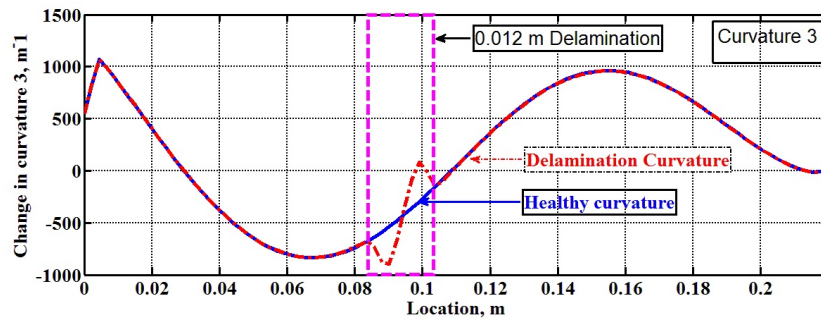


Figure 3.11: Quasi Curvature 3

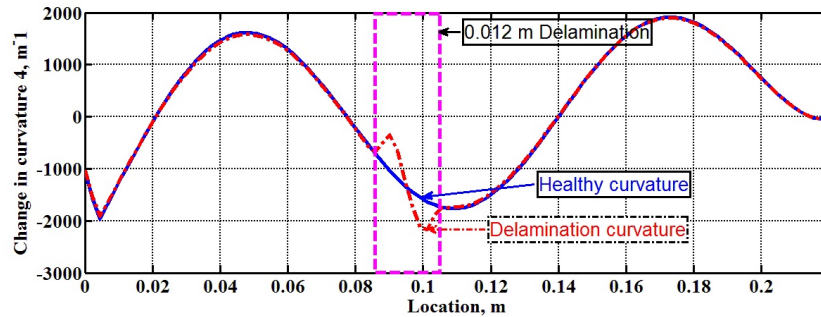


Figure 3.12: Quasi Curvature 4

3.5 Damage Detection Algorithms based on Curvature Mode shapes

To detect the location of delamination present in composite beam damage detection algorithms are applied to mode shape data from Rucevskis paper [19]. After applying damage detection algorithm it is found that mode shape curvature (MSC) and mode shape curvature square (MSCS) damage detection algorithms are most suitable to locate the delamination.

3.5.1 Mode shape (MS) damage index

It represents the difference between mode shape of healthy and damage structures

$$\Delta u_i = |u_i^d - u_i| \quad (3.1)$$

where u_i^d and u_i are mode shapes of delaminated and healthy structures and i indicates the node number. After averaging the sum of all mode shapes, average (MS) damage index is calculated as

$$MS_i = \frac{1}{N} \sum_{n=1}^N (\Delta u_i)_n \quad (3.2)$$

where N is total number of modes extracted

3.5.2 Mode shape slope (MSS) damage index

This algorithm uses change in mode shape slope by taking first derivative of mode shape

$$\Delta u'_i = |u_i'^d - u'_i| \quad (3.3)$$

By averaging all mode shape slope, average (MSS) damage index is calculated as

$$MSS_i = \frac{1}{N} \sum_{n=1}^N (\Delta u'_i)_n \quad (3.4)$$

3.5.3 Mode shape curvature (MSC) damage index

This algorithm indicates the location of delamination is assessed by difference in mode shape curvature between healthy and damage and is given as

$$\Delta u''_i = |u_i''^d - u''_i| \quad (3.5)$$

By averaging all mode shape curvature, average (MSC) damage index is calculated as

$$MSC_i = \frac{1}{N} \sum_{n=1}^N (\Delta u''_i)_n \quad (3.6)$$

3.5.4 Mode shape curvature square (MSCS) damage index

This MSCS damage index is defined as

$$\Delta u_i''^2 = |u_i''^{d2} - u_i''^2| \quad (3.7)$$

By averaging all mode shape curvature square, average (MSCS) damage index is calculated as

$$MSCS_i = \frac{1}{N} \sum_{n=1}^N (\Delta u_i''^2)_n \quad (3.8)$$

All of the damage detection algorithms mentioned above are indicating the damage location but out of all algorithms, mode shape curvature square damage index method is best suitable for locating the damage. Figure 3.13 shows mode shape curvature damage index for quasi-isotropic laminate $[45/-45/90/0]_s$ for mode 1 where maximum peak shown by barchart in the range of 0.08 to 0.09 m. Eventually for first mode some noise is present along the length direction. Figure 3.14 shows mode shape curvature damage index for mode 2 and Fig. 3.15 shows the mode shape curvature damage index for mode 3. Individually, for each mode MSC algorithm can be applied but to avoid the noise average mode shape curvature damage index is plotted for all modes as shown in Fig. 3.16 where one can see the exact location of damage present in composite beam at respective position of delamination from 0.089 to 0.101 m.

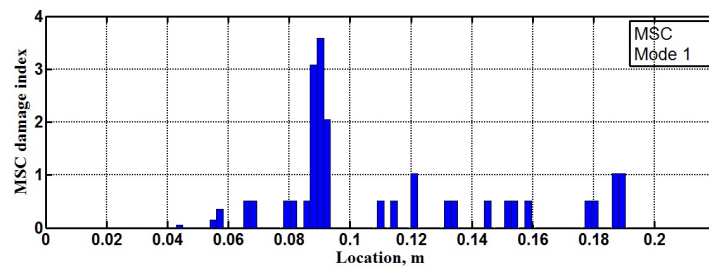


Figure 3.13: MSC 1 for quasi-isotropic GFRP $[45/-45/90/0]_s$ laminate using FEA

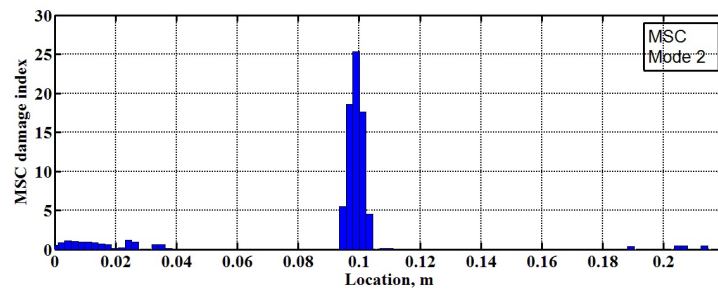


Figure 3.14: MSC 2 for quasi-isotropic GFRP $[45/-45/90/0]_s$ laminate using FEA

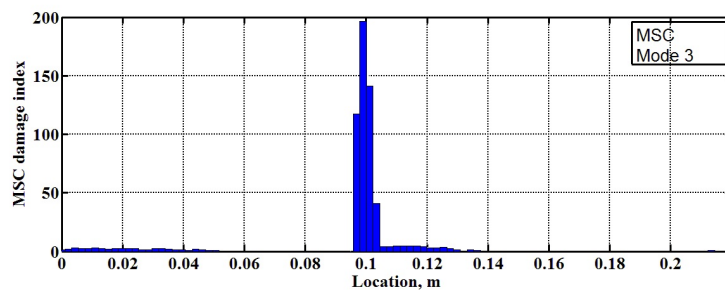


Figure 3.15: MSC 3 for quasi-isotropic GFRP $[45/-45/90/0]_s$ laminate using FEA

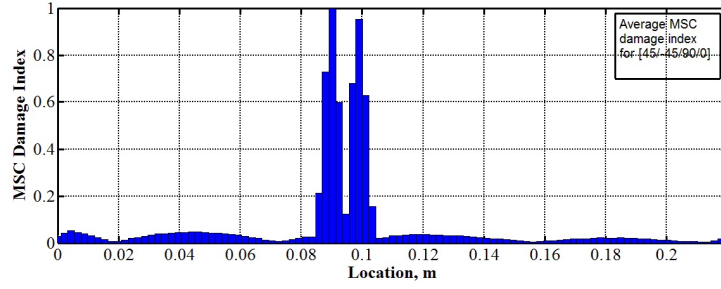


Figure 3.16: Average MSC for quasi-isotropic GFRP $[45/-45/90/0]_s$ laminate using FEA

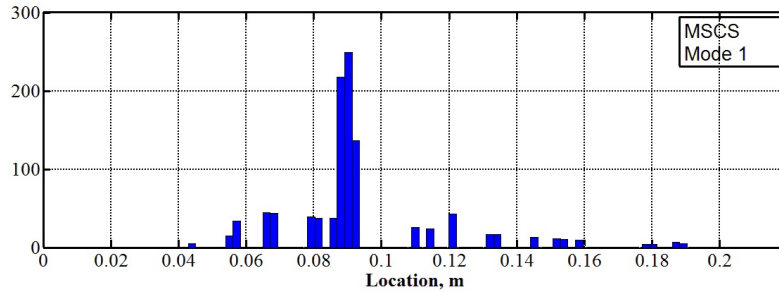


Figure 3.17: MSCS 1 for quasi-isotropic GFRP $[45/-45/90/0]_s$ laminate using FEA

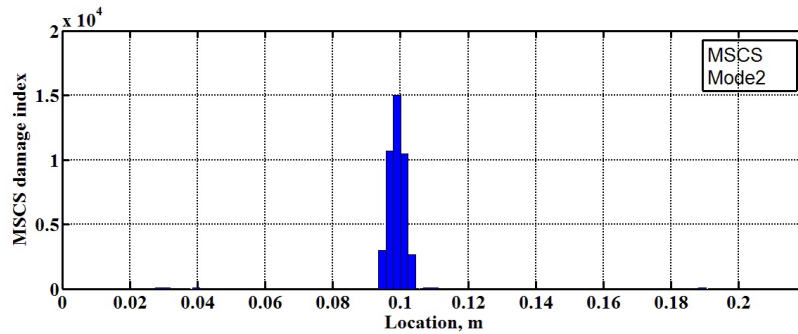


Figure 3.18: MSCS 2 for quasi-isotropic GFRP $[45/-45/90/0]_s$ laminate using FEA

Similarly, Fig. 3.17 shows mode shape curvature square damage index for quasi-isotropic $[45/-45/90/0]_s$ laminate for mode 1 where first mode contains noise along the length direction. Figure 3.18 shows mode shape curvature square damage index for mode 2 and Fig. 3.19 shows the mode shape curvature square damage index for mode 3. To avoid the unwanted noise average mode shape curvature square damage index is calculated as shown in Fig. 3.20. Normalization of average mode shape curvature square damage index represents exact location of delamination from 0.089 to 0.101 m. Thus, it concludes that mode shape curvature square (MSCS) damage index algorithm is suitable for locating the damage present in the structure.

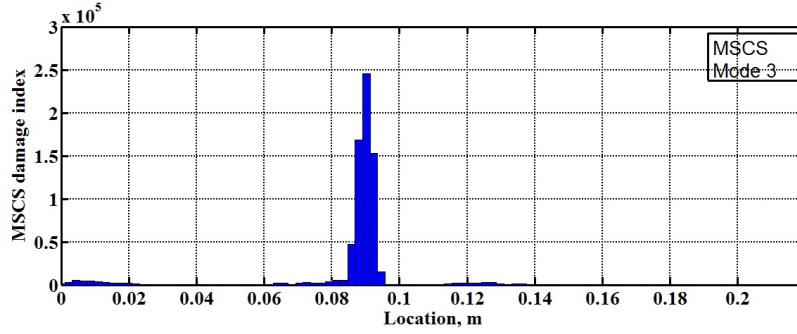


Figure 3.19: MSCS 3 for quasi-isotropic GFRP $[45/-45/90/0]_s$ laminate using FEA

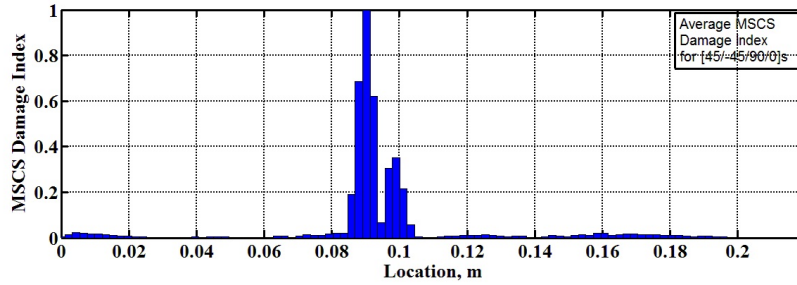


Figure 3.20: Average MSCS for quasi-isotropic GFRP $[45/-45/90/0]_s$ laminate using FEA

3.6 Damage Location

For locating the delamination experimentally curvature mode shape information is used. As in previous section various damage detection algorithms are applied to modal data obtained from FE analysis. But those algorithms are not suitable for locating the damage to experimental mode shape data. Since, experimentally obtained modal data contains noise. To identify the exact damage location is difficult using above algorithms. For locating the damage experimentally curvature damage index is preferred and is validated with FEA.

3.6.1 Curvature Damage Index

Curvature damage index is obtained by change in curvature mode shape of delaminated and healthy curvature upon healthy curvature. This ratio represents the magnitude of damage measure on ordinate axis versus damage location along abscissa axis.

$$\Delta v_i'' = \frac{|v_i''^d - v_i''|}{v_i''} \quad (3.9)$$

where $v_i''^d$ and u_i'' are curvature mode shapes of delaminated and healthy structures respectively and i indicates the node number. After averaging the all mode shape curvatures the damage index (CDI) is calculated as

$$CDI_i = \frac{1}{N} \sum_{n=1}^N (\Delta v_i'')_n \quad (3.10)$$

where N is total number of modes extracted. Figure 3.21 shows the damage location for quasi-isotropic $[45/-45/90/0]_s$ laminate using LDV where peak value of barchart shows the location of damage. Since first mode contains noise. To avoid the unwanted noise averaging of extracted modes is preferred. As shown in Fig. 3.22 show the peak at damage location. After averaging of these modes, normalised curvature damage index is shown in Fig. 3.23 obtained using experimental data.

To validate the damage location obtained by LDV with FEA. Curvature damage index algorithm is applied to mode shape data obtained by FEA. Figure 3.24 shows the damage location for quasi-isotropic $[45/-45/90/0]_s$ laminate using FEA where peak value of barchart at free end contains noise. Fig. 3.25 shows the peak at 0.1 m along damage location. To avoid the unwanted noise average curvature damage index is calculated. As shown in Fig. 3.26 shows the peak at damage location obtained using FEA. After comparing Fig. 3.23 and Fig. 3.26 one can conclude that damage locations found by LDV and FEA using curvature damage index algorithm are qualitatively comparable.

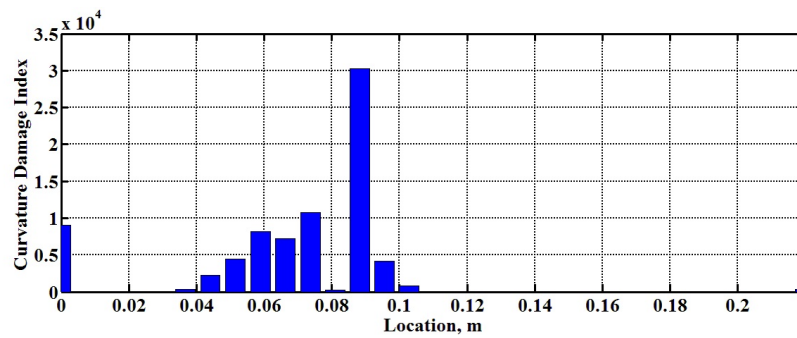


Figure 3.21: CDI 1 for quasi-isotropic GFRP $[45/-45/90/0]_s$ laminate using LDV

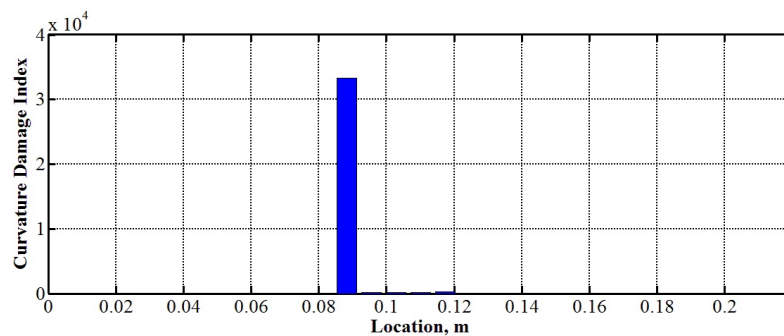


Figure 3.22: CDI 2 for quasi-isotropic GFRP $[45/-45/90/0]_s$ laminate using LDV

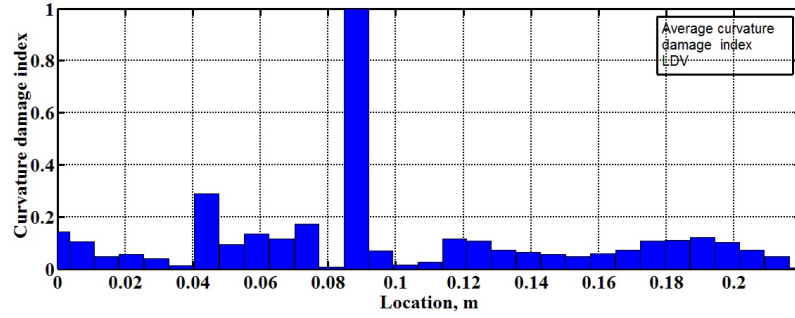


Figure 3.23: Average CDI for quasi-isotropic GFRP $[45/-45/90/0]_s$ laminate using LDV

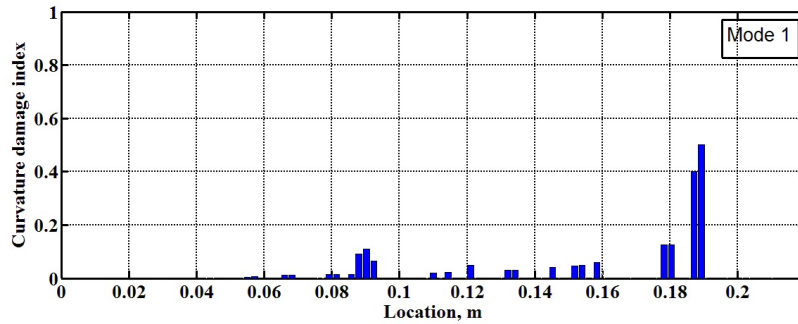


Figure 3.24: CDI 1 for quasi-isotropic GFRP $[45/-45/90/0]_s$ laminate using FEA

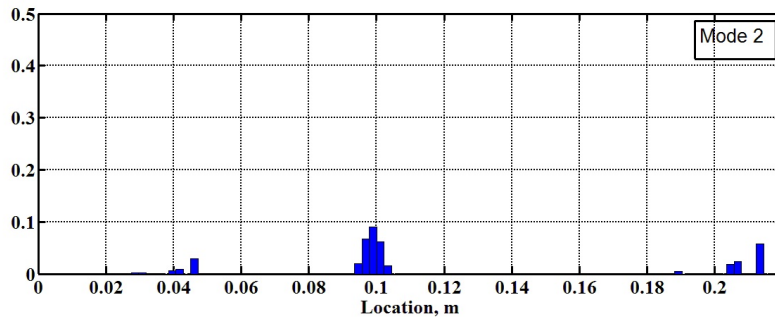


Figure 3.25: CDI 2 for quasi-isotropic GFRP $[45/-45/90/0]_s$ laminate using FEA

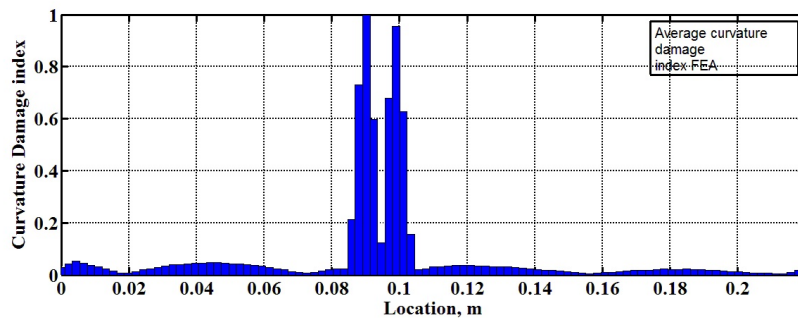


Figure 3.26: Average CDI for quasi-isotropic GFRP $[45/-45/90/0]_s$ laminate using FEA

3.7 Closure

Experimentally, change in natural frequencies are observed in delamination beams are validated with FEA. Shift in natural frequencies and mode shapes are giving information about the presence of damage. Mode shapes for healthy and delamination specimen are compare qualitatively for different configuration using FEA and LDV. To locate the delamination present in composite beam different damage detection algorithms are applied. Mode shape curvature square damage detection algorithm is most suitable for locating delamination. Experimental damage location is found out by curvature damage index algorithm and compare qualitatively with FEA.

Chapter 4

Conclusion and Recommendations for Future Work

4.1 Concluding Remarks

This thesis focuses on the detection and location of delamination type of damage present in the composite beam by extracting the modal parameters obtained from the modal analysis test on the GFRP specimens using experimental and numerical approach. The experimental approach comprises of testing of GFRP composite laminated beams with an embedded through-width delamination having 12 mm width at centre position of the beam. Numerical simulation carried out using FEM to study effect of delamination on modal parameter using SOLID185 and SHELL181 elements are matching with analytical model. Finite element (FE) analysis is performed to locate the delamination and the validity of the damage detection algorithms is verified. Experimentally as well as numerically it is observed that there is frequency change in delamination specimen as compared to healthy one. Experimentally it is observed that natural frequency depends on thickness of laminate and stacking sequence used and boundary applied condition. As we double the number of layers of the composite specimen hence frequencies doubled. Due to presence of delamination reduces stiffness and strength of the structure and hence affects modal parameters such as natural frequency and mode shapes. By using this modal information location of delamination is qualitatively compare by applying damage detection algorithms. For locating the delamination mode shape curvature square damage index algorithm is preferred. Experimentally damage location is found by using curvature damage index algorithm and further validated with FEA. Laser Doppler Vibrometer can applied to modal analysis of aircraft components, automotive parts, car bodies etc.

4.1.1 Modal Analysis

The modal analysis test is conducted on healthy and damage specimens and the response plots are acquired in the form of modal parameters such as natural frequencies and mode shapes. The LDV system provides the output in the form of displacement mode shapes, from which the curvature mode shapes are calculated by numerical differentiation process. The displacements mode shape and curvature mode shape data is used to locate the delamination type of damage.

4.1.2 Damage detection Algorithms

Damage detection algorithms are applied to the data extracted from the vibration testing of the composite beam specimens. Such as difference in delaminated and healthy mode shapes (MS), mode shape slope (MSS), mode shape curvature (MSC), mode shape curvature square (MSCS). The results of delamination detection in the composite beams shows the significant effect of boundary conditions on the damage identification. Experimentally it is found that the delamination is not easier to be detected in the cantilever boundary condition. The displacement mode shapes of the cantilever composite beam directly obtained from the LDV system and numerical FE simulations are used in the damage detection algorithms and they are effective of identification the location of the delamination.

4.2 Recommendations for Future Work

In this research, the study of damage detection in composite beams is conducted. Some observations are carried out during vibration test such that mesh-grid defined on the specimen surface should be of high mesh density to improve the proposed damage detection methodology. Due to presence of delamination in composite beam it is impossible to implement the standard damage index method such as strain energy based damage index method (SDI). SDI method is not applicable for delamination problem since it is applicable for crack detection problems. Therefore some algorithms need to be developed for estimating damage index for delamination type of problems. Also one can extend this problem for plate type structure where delamination may be present with different size and at different locations. More research on different types of damage at the different locations using the proposed damage detection algorithms and sensor systems should be conducted. Repetition and averaging of the tests may provide better results and gives an idea of handling the equipment. Thus more repeated experiments should be carried out with averaging the magnitude of excitation. For future work i would like to suggest that before conducting the experiment on LDV equipment, first perform the experiment without clamping the specimen and check vibrations of fixture which is mounted on shaker. By doing this preliminary test you will get an idea of performing the experiment.

References

- [1] D. Balageas, C.-P. Fritzen, and A. Güemes. Structural health monitoring, volume 493. Wiley Online Library, 2006.
- [2] R. M. Jones. Mechanics of composite materials, volume 1. McGraw-Hill New York, 1975.
- [3] S. Gopalakrishnan, M. Ruzzene, and S. Hanagud. Computational techniques for structural health monitoring. Springer Science & Business Media, 2011.
- [4] W. Lestari, P. Qiao, and S. Hanagud. Curvature mode shape-based damage assessment of carbon/epoxy composite beams. *Journal of intelligent material systems and structures* 18, (2007) 189–208.
- [5] T. H. Ooijevaar. Vibration based structural health monitoring of composite skin-stiffener structures. Universiteit Twente, 2014.
- [6] S. S. Kessler, S. M. Spearing, M. J. Atalla, C. E. Cesnik, and C. Soutis. Damage detection in composite materials using frequency response methods. *Composites Part B: Engineering* 33, (2002) 87–95.
- [7] Z. Zhang, K. Shankar, T. Ray, E. V. Morozov, and M. Tahtali. Vibration-based inverse algorithms for detection of delamination in composites. *Composite Structures* 102, (2013) 226–236.
- [8] P. Cawley and R. Adams. The location of defects in structures from measurements of natural frequencies. *The Journal of Strain Analysis for Engineering Design* 14, (1979) 49–57.
- [9] P. Cawley and R. D. Adams. A vibration technique for non-destructive testing of fibre composite structures. *Journal of Composite Materials* 13, (1979) 161–175.
- [10] G. C. Pardoen. Effect of delamination on the natural frequencies of composite laminates. *Journal of composite materials* 23, (1989) 1200–1215.
- [11] A. Pandey, M. Biswas, and M. Samman. Damage detection from changes in curvature mode shapes. *Journal of sound and vibration* 145, (1991) 321–332.
- [12] M. Pavier and M. Clarke. Experimental techniques for the investigation of the effects of impact damage on carbon-fibre composites. *Composites science and technology* 55, (1995) 157–169.
- [13] C. R. Farrar and S. W. Doebling. An overview of modal-based damage identification methods. In Proceedings of DAMAS Conference. Citeseer, 1997 269–278.

- [14] H. Luo and S. Hanagud. Dynamics of delaminated beams. *International Journal of Solids and Structures* 37, (2000) 1501–1519.
- [15] Y. Zou, L. Tong, and G. Steven. Vibration-based model-dependent damage (delamination) identification and health monitoring for composite structures a review. *Journal of Sound and vibration* 230, (2000) 357–378.
- [16] S. Lee, T. Park, and G. Z. Voyiadjis. Vibration analysis of multi-delaminated beams. *Composites Part B: Engineering* 34, (2003) 647–659.
- [17] C. N. Della and D. Shu. Vibration of delaminated composite laminates: A review. *Applied Mechanics Reviews* 60, (2007) 1–20.
- [18] V. Tita, J. De Carvalho, and D. Vandepitte. Failure analysis of low velocity impact on thin composite laminates: Experimental and numerical approaches. *Composite Structures* 83, (2008) 413–428.
- [19] S. Rucevskis and M. Wesolowski. Identification of damage in a beam structure by using mode shape curvature squares. *Shock and Vibration* 17, (2010) 601–610.
- [20] W. Fan and P. Qiao. Vibration-based damage identification methods: a review and comparative study. *Structural Health Monitoring* 10, (2011) 83–111.
- [21] O. K. Ihesiulor, K. Shankar, Z. Zhang, and T. Ray. Delamination detection with error and noise polluted natural frequencies using computational intelligence concepts. *Composites Part B: Engineering* 56, (2014) 906–925.
- [22] M.-H. Shen and J. Grady. Free vibrations of delaminated beams. *AIAA journal* 30, (1992) 1361–1370.